This is to certify that the

thesis entitled

An Approach to probe The Glucose-6-phosphate Binding Site of Rat Brain Hexokinase by Photoaffinity Labeling

presented by

Hui-Jane Lu

has been accepted towards fulfillment
of the requirements for

MASTER degree in SCIENCE

John E. Wilson

Major professor

Date 12-10-91

AN APPROACH TO PROBE THE GLUCOSE-6-PHOSPHATE BINDING SITE OF RAT BRAIN HEXOKINASE BY PHOTOAFFINITY LABELING

By

Hui-Jane Lu

A THESIS

submitted to
Michigan State University
in partial fulfillment of the requirements
for the degree of

MASTER Of SCIENCE

Department of Biochemistry

1991

ABSTRACT

AN APPROACH TO PROBE THE GLUCOSE-6-PHOSPHATE BINDING SITE OF RAT BRAIN HEXOKINASE BY PHOTOAFFINITY LABELING

By

Hui-Jane Lu

Five glucose-6-phosphate (G6P) analogs were synthesized and their structures were confirmed by ^{1}H-NMR, FT-IR and FAB-mass spectrometry. Inhibition studies on rat brain hexokinase indicated that modifications of G6P at the β anomeric position (C1, equatorial) of the glucopyranose ring with either azido or benzyl groups result in loss of inhibitory function. However, mixtures of α (C1, axial) and β anomers of either 1-azidoethyl G6P or 1-benzyl G6P still retain their inhibitory effectiveness with α presumably being the active inhibitory form. Substitution of a hydroxyl group at C3 with an azido group, drastically alters the inhibitory activity.

Since 1-azidoethyl-G6P did not label brain hexokinase after photolysis and an attempt to make α-1-azidobenzyl-G6P was not successful, 3-azido-G6P was used in photolabeling of this enzyme. However, there was nonspecific labeling and efforts at reducing it were not successful. The 50 kDa fragment at the N-terminus of hexokinase, was about twice as densely labeled as the C-terminal fragment, with no protection effect by G6P. Thus, it was impossible to demonstrate specific labeling of the inhibitory site in the 50 kDa fragment. Possible explanations are given for this unusual observation.

ACKNOWLEDGEMENTS

Above all I wish to thank Dr. John Wilson for his guidance and support in my thesis work. I also wish to thank Dr. Rawle Hollingsworth and Dr. Shelagh Ferguson-Miller for many discussions and suggestions.

I am grateful to the mass spectrometry facility for their help in getting mass spectra, and also to Jeff Zaleski in chemistry department for his help in using laser. My thanks also go to Al Smith and Annette Thelen, who kindly taught me some lab techniques when I needed. I will not forget Anita, Dave, Hector, Firoz, and Madhu for their friendly companionship in this lab.

Finally, I would address my deep gratefulness to my beloved parents for their understanding and support during these years of my overseas study, also to my dear friends for their endless sharing and encouragement.

TABLE OF CONTENTS

LIST OF TABLES

LIST OF FIGURES

LIST OF SCHEMES

LIST OF ABBREVIATIONS

BSA	bovine serum albumin
DCC	1,3-dicyclohexylcarbodiimide
FT-IR	Fourier transform-infrared spectrometry
FT-NMR	Fourier transform-nuclear magnetic resonance spectrometry
G6P	glucose-6-phosphate
HK	hexokinase
negative-FAB-mass	negative-fast atom bombardment-mass spectrometry
PAGE	polyacrylamide gel electrophoresis
SDS	sodium dodecyl sulfate
TCA	trichloroacetic acid
TEA	triethanolamine

INTRODUCTION

Brain hexokinase

Hexokinase (ATP:D-hexose-6-phosphotransferase, EC 2.7.1.1.) is the first enzyme of the glycolytic pathway and catalyses the conversion of glucose and Mg-ATP into glucose-6-phosphate (G6P) and Mg-ADP. There are four known hexokinases from mammals. They are distinguished on the basis of charge (Type I, II, III, IV). These four isozymes also differ in their tissue distribution and the kinetic parameters (i.e. K_m, K_i) that reflect a complex regulation of glucose metabolism in mammalian tissues (1).

Type I hexokinase is found to be the predominant isozyme in brain and it binds to the outer mitochondrial membrane reversibly in a G6P-sensitive manner (2-4). Brain hexokinase activity is inhibited by its reaction product, G6P, and also regulated by several nucleotides and inorganic phosphate (5-7).

Binding of various ligands to brain hexokinase induces conformational changes of the enzyme (8). The different conformations induced by binding of various ligands have been compared by determination of the protection against proteolysis, heat and chemical modifications. These comparisons indicate not only binding but also the induction

of conformational change are necessary for the ligands to serve as good substrates or inhibitors of brain hexokinase (9).

Structural domains of hexokinase and the structure-function relationship

Rat Type I hexokinase is composed of a single polypeptide chain with molecular weight of 100 kDa. It has been cleaved with limited tryptic digestion to yield discrete fragments, in order from the N-terminus of the enzyme, with molecular masses of 10 kDa, 50 kDa and 40 kDa, as depicted below.

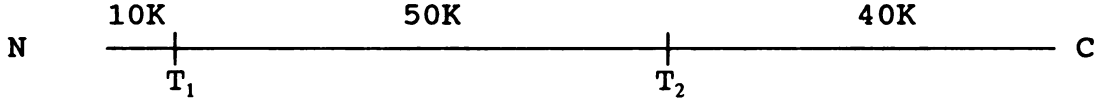

T_1, T_2 = tryptic cleavage sites

Each fragments seemed associated with specific functions. The N-terminal 10 kDa fragment is known to include an N-terminal hydrophobic segment required for specific and reversible interaction with the outer mitochondrial membrane (11). The 40 kDa fragment at the C-terminus has been shown to contain both glucose and ATP substrate binding sites based on affinity labeling experiments (12,13). Isolation and kinetic analysis of a 48 kDa fragment representing the C-terminal half of hexokinase further demonstrated that this fragment accounts for all the

catalytic activity of the enzyme (14). The observation that G6P protected a 52 kDa fragment, representing the N-terminal half of the enzyme, from denaturation and proteolysis, strongly suggested that the G6P binding site was located in the N-terminal half (15). However, the precise location the G6P binding site within this fragment still remains unknown.

Regulation of brain hexokinase activity by G6P

As mentioned previously, brain hexokinase is regulated by its reaction product, G6P. On the basis of noncompetitive nature of G6P inhibition with respect to glucose and the observation of dissimilar specificities for hexose and hexose-6-phosphate binding sites (16,17), an allosteric regulatory site which is spatially distinct from the catalytic site for G6P was proposed (16). However, the competitive manner of G6P inhibition versus ATP does not rule out the possibility that G6P binding site overlaps the substrate ATP binding site so that G6P and ATP directly compete with each other on binding at the overlapping site (18,19).

The molecular basis of the inhibition of hexokinase by G6P is still debated by different investigators so far (18-21). Recently, Jarori et al. (22) attempted to resolve the locations of binding sites of G6P and glucose with respect to a previously identified divalent-cation binding site by NMR studies. They deduced the existence of a G6P binding

site in close proximity (within 2 nm) to the glucose binding site. However, based on spatial consideration of the catalytic site at C-terminus and the regulatory site at N-terminus of brain hexokinase, Hutny and Wilson (23) argued the G6P binding site found by Jarori et al. at high experimental concentrations of G6P (3.33 to 9.5 mM) was in fact a low affinity site instead of the high affinity regulatory site (K_d= 0.01 mM) found in the earlier G6P binding studies.

Since the crystallographic structures of hexokinase-ligand complexes have not been obtained, a more complicated relationship between the catalytic site and the regulatory site can always be imagined. For example, the G6P binding site and the ATP binding site might be spatially far from each other in the absence of ligands. But on G6P binding, the ligand (G6P) may induce a conformational change, which brings its phosphate moiety to the γ-phosphate position of the ATP binding site and therefore prevents ATP from binding.

The regulatory site where G6P binds requires further definition. Identification of the amino acids directly involved in that regulatory site would help in resolving this question.

<u>The specificity for the G6P inhibition site of brain hexokinase</u>

Studies on the specificity for the G6P inhibitory site were initiated by Crane and Sols (16) and further investigated in other laboratories (24,25). These studies concerned determination of the inhibitory effectiveness of a series of hexose-6-phosphates and related compounds as competitive (vs. ATP) inhibitors of hexokinase. Based on their studies of twenty-five compounds (16), Crane and Sols drew the conclusion that only the hydroxyl groups on carbons 2 and 4 and the phosphate at carbon 6 may be attaching groups in the enzyme-inhibitor complex so that substitutions or configurational changes on these carbons resulted in loss of inhibitory ability. And they also suggested a pyranose structure is required, inasmuch as when no ring is present (e.g. gluconate-6-phosphate), inactivity results. Although substitution of the hydroxyl group on carbon 3 with a proton or change in the configuration at this carbon (i.e. allose-6-phosphate) do not result in complete loss of the inhibitory activity, still the K_i values increase to about 20 to 50 fold that of G6P. The later studies by Rose et al. (24) indicated that although both anomers of G6P were about equally active inhibitors, a substitution at the C1 equatorial, β, position by groups larger than a proton and smaller than a monophosphate may prevent binding to the inhibitory site. Wilson and Chung (25) further studied the essentiality of the divalent phosphate moiety at carbon 6 and the enhancement of the inhibitory activity by

substitution of the oxygen atom in the pyranose ring of G6P with a sulfur atom.

The effect of G6P and related compounds on phosphorylation by brain hexokinase is summarized in Table I.

The photochemistry of azides and their application in active site studies

As stated by Reiser and Wagner (26), the salient feature of the photochemistry of organic azides is the elimination of a molecular nitrogen from the azido group on irradiation.

$$RN_3 + h\nu \text{ ---------->} RN + N_2$$

The molecular fragment RN is the primary product of this process and generally called nitrene. Nitrenes are chemically reactive radical species which immediately undergo the subsequent reactions to form more stable products. Such reactions include the rearrangement of nitrene itself, insertion of nitrene into a single bond (usually C-H, O-H, and N-H) or addition to multiple bonds (double or triple bonds) of other molecules.

The organic azides (RN_3) can be classified into two classes according to the chemical structures of R. Those azides with the azido groups directly attached to the aromatic rings of R groups are called aryl azides or

TABLE I

SPECIFICITY FOR G6P INHIBITION SITE OF BRAIN HEXOKINASE

Modification at carbon No.	Compound	Percent Inhibition at the indicated concentration (mM)	K_i (mM)	K_i / K_i(G6P)'	Reference
0	G6P		0.026; 0.4*	1	50 16
1	1-deoxy-G6P		0.02	1	24
1	α-CH_3-G6P		0.13	5	24
1	β-CH_3-G6P		> 5	> 190	24
1	α-Glucose-1,6,-P_2		0.11; 0.7*	4.2; 1.8*	24 16
1	β-Glucose-1,6,-P_2	0 (1 mM)			16
2	Mannose-6-P	0 (8.5 mM)			16
2	2-deoxy-G6P	0 (1 mM)			16
2	Glucosamine-6-P	0 (1.5 mM)			16
3	Allose-6-P		7.0*	17.5*	16
3	3-deoxy-G6P		20.0*	50*	16
4	Galactose-6-P	0 (20 mM)			16
No ring	Gluconate-6-P	0 (1 mM)			16
5	5-Thio-G6P		0.0004	0.04	25

6	Glucose-6-fluorophos-phate	19 (0.75 mM)			25
6	Glucose-6-Sulfate	30 (0.8 mM)			25

* The K_i values were derived from reference (16).

Because the K_i value of G6P derived from (16) varied from (24) and (25), the K_i / K_i (G6P) were calculated for easier comparison of the relative inhibitory effectiveness of these G6P analogs to the brain hexokinase activity.

aromatic azides. And those which are not classified as aromatic azides are included in the class of aliphatic azides. These two classes of azides differ not only in their structures but also in their photochemical properties. With the aliphatic nitrenes (generated from their corresponding azides), the insertion reaction is generally much slower than the faster hydrogen migration process which results in formation of imines. Only when hydrogen migration and other rearrangements are inhibited do insertions become important. In contrast, the aromatic nitrenes favor the insertion or addition process (26).

Due to their ability to be converted into highly reactive nitrenes upon photolysis, organic azides are useful as photolyzable reagents for site-labeling studies of macromolecules (27). A photolabile azide is anchored to the macromolecule and photolysis of the complex then leads to the generation of a highly reactive nitrene that, by reacting rapidly with the immediate environment, labels the macromolecule specifically at the binding site. This technique has been widely used in labeling of a number of active sites of macromolecules and is referred to as photoaffinity labeling.

Quite a few aromatic azides have been successfully used as photoaffinity labeling reagents in biological systems. For example, nucleotide analogs were used in labeling of the active sites of F_1-ATPase (28) and hexokinase (13) or the

allosteric site of cAMP-dependent protein kinase C (29); alternatively, some ligands without aromatic structures were modified with azidophenyl groups and then used in labeling of binding sites of antibodies (30,31), xylosidase (32), and myosin ATPase (33). Many other successful examples of photoaffinity labeling are to be found in recent publications.

In contrast to the aromatic azides, the application of aliphatic azides is seldom found in the literature. The possible reasons for less usefulness of aliphatic azides for affinity labeling purposes are that their nitrene intermediates are more susceptible for rearrangement and also the aliphatic azides are photolyzed relatively slowly (low quantum yield or low extinction coefficient) in comparison to the aryl azides (34).

Consideration of the approaches taken for elucidating the G6P-binding of brain hexokinase

The identification and structural characterization of the G6P-binding site of brain hexokinase is essential to understanding the molecular basis of how G6P inhibits the hexokinase activity. As stated previously, the N-terminal 50 kDa domain is believed to be where the G6P-binding site resides (15), but amino acids directly interacting with G6P in the binding site are still unknown.

Different approaches are capable of providing

information about ligand-binding sites of proteins. Those which are widely known include affinity labeling, X-ray crystallography, NMR spectroscopy, ESR spectroscopy, Raman spectroscopy, fluorescence spectroscopy, and more recently, site-directed mutagenesis. But each of these has certain limitations and cannot necessarily be applied to all kinds of proteins.

X-ray crystallography might be the one which gives molecular information of ligand-binding sites in greatest detail. Efforts have been made by some crystallographers, but brain hexokinase has not yet been crystallized. Two dimensional NMR spectroscopy is capable of yielding structures of small proteins (approximately 10 kDa) in solutions (35), But brain hexokinase, with molecular weight 100 kDa, is beyond the size limitation for NMR studies. Raman spectroscopy and fluorescence spectroscopy, cannot be used to unambiguously identify specific amino acids of proteins which directly interact with the binding ligands, so these latter two spectroscopic methods are not considered at this point.

Affinity labeling, which has been applied in the elucidation of the catalytic site structure for brain hexokinase is again considered for probing the regulatory site of the same enzyme. The labeling compounds usually resemble substrates or effectors in structure providing specificity, and covalently react with amino acid(s) within

the ligand binding sites. Identification of the labeled amino acids then locates the ligand binding sites within the protein. But classic affinity labeling generally depends on the presence of appropriately positioned reactive functional groups on the enzyme (27). Such a requirement is frequently satisfied at catalytic sites because the electrophilic and nucleophilic groups involved in catalysis may be present there. However, for the allosteric binding site where catalysis does not take place, this requirement is not necessarily met. Photoaffinity labeling reagents, using very reactive radical species generated upon photolysis, are known in many cases to react readily with the immediate environment (27). So on binding to the proteins, they react with those amino acids in the closest proximity without discrimination. For the purpose of probing G6P-binding site of hexokinase, this approach might be worth trying.

Goal and approach

As stated previously, the molecular basis for the inhibition of brain hexokinase activity by G6P is not clear. An understanding of the exact location of the G6P binding site and its structure is possibly a key to resolve this question. Also, different approaches used in studying ligand binding sites were considered for their feasibility in probing the G6P binding site of brain hexokinase, and photoaffinity labeling seemed of potential value.

Since G6P itself is not photoactivatable, it must be

modified with a group, such as an azido group, which is able to generate radical species upon photolysis. This modified G6P should retain the specificity for the G6P binding site and its inhibitory activity should be as close to that of G6P as possible. The following criteria are very important for making an effective labeling reagent:

a. The synthesized G6P analog must retain the specificity and inhibition properties seen with G6P itself (i.e. be competitive versus substrate ATP). This is evaluated by inhibition studies.

b. Due to modification, the G6P analog might have its inhibitory effectiveness different from that of G6P to the brain hexokinase. However, this difference should be as small as possible. This is reflected by the K_i value (competitive inhibition vs. ATP). A lower K_i means the compound inhibits the enzyme more effectively so that a lower concentration of the compound can be used for affinity labeling of the G6P binding site and the problem of unspecific labeling is therefore diminished.

Based on our knowledge about the specificity of the G6P binding site of brain hexokinase (Table I), only two candidate positions of G6P, (at carbons 1 and 3), can be modified with only modest change of inhibitory effectiveness. So in the present work, G6P was modified only on carbon 1 or carbon 3 of the pyranose ring. After chemical synthesis, the structures of the synthesized analogs were

confirmed and their inhibitory effectiveness evaluated by kinetic studies. An azido G6P derivative, which satisfies most of the above criteria, might be useful as a photoaffinity labeling reagent in probing the G6P binding site of brain hexokinase.

MATERIALS AND METHODS

Materials

Trypsin, G6P dehydrogenase, pyruvate kinase-lactate dehydrogenase (PK-LDH enzyme), yeast hexokinase, bovine serum albumin, G6P (disodium salt), 1,2:5,6-di-O-isopropylidene-α-D-allofuranose, orcinol, and sodium azide were purchased from Sigma Chemical Co.(St. Louis, MO). Hydrogen bromide (30% in acetic acid), mercury (II) cyanide and 1,3-dicyclohexylcarbodiimide were products of Aldrich Chemical Co.(Milwakee, WI). Trifluoroacetic anhydride, p-toluene-sulfonic acid and benzyl alcohol were obtained from J.T. Baker Inc.(Phillipsburg, NJ). Trifluoroacetic acid and phosphorus pentoxide (P_2O_5) were purchased from EM Science Co. (Cherry Hill, NJ). Formic acid (88%) and N,N-dimethylformamide were products of Fisher Scientific Co. (Fair Lawn, NJ). Acetonitrile was obtained from Baxter Healthcare Co. (Muskegon, MI). [γ-^{32}P] ATP was purchased from ICN Pharmaceuticals, Inc.(Irvine, CA). The Bio-gel P2 and ion exchange resins AG 50W-X4 and AG 1-X8 (200-400 mesh) were obtained from Bio-Rad Laboratories (Rockville Center, NY). The TLC plates was a product of Whatman International, Ltd. (Maidstone, England). The Safety-Solve liquid scintillant was from Research Products International Corp.

(Mount Prospect, IL). Dry pyridine was prepared by distillation of the commercial product from potassium hydroxide.

Methods

Purification of rat brain hexokinase

Rat brain hexokinase was prepared according to Wilson (36).

Protein assay

A molar extinction coefficient of 5.1×10^4 cm^{-1} M^{-1} at 280 nm was used to determine hexokinase concentration (37). Trypsin solutions were freshly prepared in 1 mM HCl and the concentration determined from absorbance at 280nm based on an absorbance of 1.43 for a 1 mg/ml solution (38).

Phosphate assay

This was done according to Ames (44). To the organic phosphate sample (0.01 to 0.1 ml in a borosilicate glass test tube), 0.03 ml 10% $Mg(NO)_3$ in ethanol was added. This sample was carefully ashed on a flame and then 0.3 ml 0.5 M HCl was added after cooling. The test tube was capped with a marble to avoid evaporation of the sample and prevent moisture from the bath from changing the sample volume while heating in a boiling water bath for 15 minutes. On cooling, 0.7 ml of phosphate assay reagent (1:6 v/v solution A:

solution B. Solution A: 10% ascorbic acid in water, Solution B: 0.42% $(NH_4)_6Mo_7O_4,4\ H_2O$ in 1N H_2SO_4) was added. This mixture was incubated at 42°C water bath for 20 minutes and then cooled before reading the absorbance at 820 nm or 800 nm. Quantitation was based on a standard curve using 0.01 to 0.08 μ mole sodium phosphate, run along with samples. The inorganic phosphate assay is done in the same way without ashing the sample in advance.

Hexokinase assay and inhibition studies

Hexokinase activity was coupled to either G6P dehydrogenase activity or pyruvate kinase-lactate dehydrogenase activity and measured spectrophotometrically. The G6P dehydrogenase-coupled hexokinase assay was performed as described by Wilson (36). For inhibition studies, hexokinase was chromatographed on Sephadex G-25 (fine) column equilibrated with 50 mM HEPES, 0.5 mM EDTA and 10 mM thioglycerol; G6P dehydrogenase and NADP stocks were prepared as described by White and Wilson for removal of sulfates and phosphates (14). Concentrations of the G6P analogs were quantitated based on phosphate assay.

In the study of 3-azido-G6P inhibition of hexokinase activity, the inhibitor itself was a substrate of G6P dehydrogenase (K_m= 1 mM) so that the G6P dehydrogenase-coupled assay could not be used and the pyruvate kinase-lactate dehydrogenase-coupled (PK-LDH) assay was used

instead. The reaction solution contained in a total volume of 0.5 ml, 2.84 mM glucose, 4.8 mM $MgCl_2$, 48 mM KCl, 38.7 mM Tris-HCl buffer, pH 8.5, 1 mM phosphoenolpyruvate, 0.12 mM NADH, 3.75 units of pyruvate kinase and 4.5 units of lactate dehydrogenase, and varied concentrations of ATP and 3-azido-G6P. After the contaminating pyruvate and ADP in the solution were used up, the reaction was initiated by the addition of hexokinase and the progress of the reaction was recorded as the decrease in absorbance at 340 nm.

Trypsin modification of native hexokinase

This was done according to Polakis and Wilson (10). Hexokinase was incubated with trypsin in 0.1 M sodium phosphate, 0.1 M glucose, 0.01 M thioglycerol, and 0.5 mM EDTA, pH 7.0, for one hour at room temperature. The protease:substrate ratio was 1:5 (w/w). Proteolysis was terminated by addition of 1 mM PMSF followed by additional incubation at room temperature for 10 minutes. Trypsin-modified hexokinase was then chromatographed on a Sephadex G-25 (fine) column equilibrated with 50 mM HEPES, 0.5 mM EDTA, and 10 mM thioglycerol, pH 7.5, for removal of glucose and phosphates. The cleaved fragments remain associated by noncovalent forces and retain many properties of the intact enzyme, as described by Polakis and Wilson (10).

Hexokinase inhibition analysis

Data from inhibition studies were analyzed using the EZ-Fit program (39).

Thin layer chromatography (TLC) and orcinol spray

TLC was done on silica gel-coated glass plates (0.25 mm layer) and developed in the solvent systems as indicated. For orcinol spray (47), 0.2 g orcinol was dissolved in 75 ml ethanol and 25 ml concentrated sulfuric acid was added. After TLC, the plates were evenly sprayed with the prepared orcinol reagent, and baked on a hot plate until the brown spots representing different sugar species were visible.

Spectroscopic analysis of synthesized G6P analogs

The synthesized G6P analogs were characterized using ^{1}H-NMR, negative-FAB-mass and FT-IR. The ^{1}H-NMR spectra were done using Varian 300 MHz VXR spectrometer. The negative-FAB-mass spectra were obtained in the Mass Spectrometry Facility, Michigan State University, and IR spectra were done using a Nicolet 710 FT-IR Spectrometer.

Synthesis of β-D-1-Azido-G6P

Scheme 1 outlines synthesis of this compound. In a -10°C NaCl/ice bath, 1.26g G6P (disodium salt) **1** was dissolved in 20 ml trifluoroacetic acid then 30 ml of acetic acid/trifluoroacetic anhydride (2:1 v/v) was added to the solution with stirring at 5°C. After 12 hours, 2.80 ml of

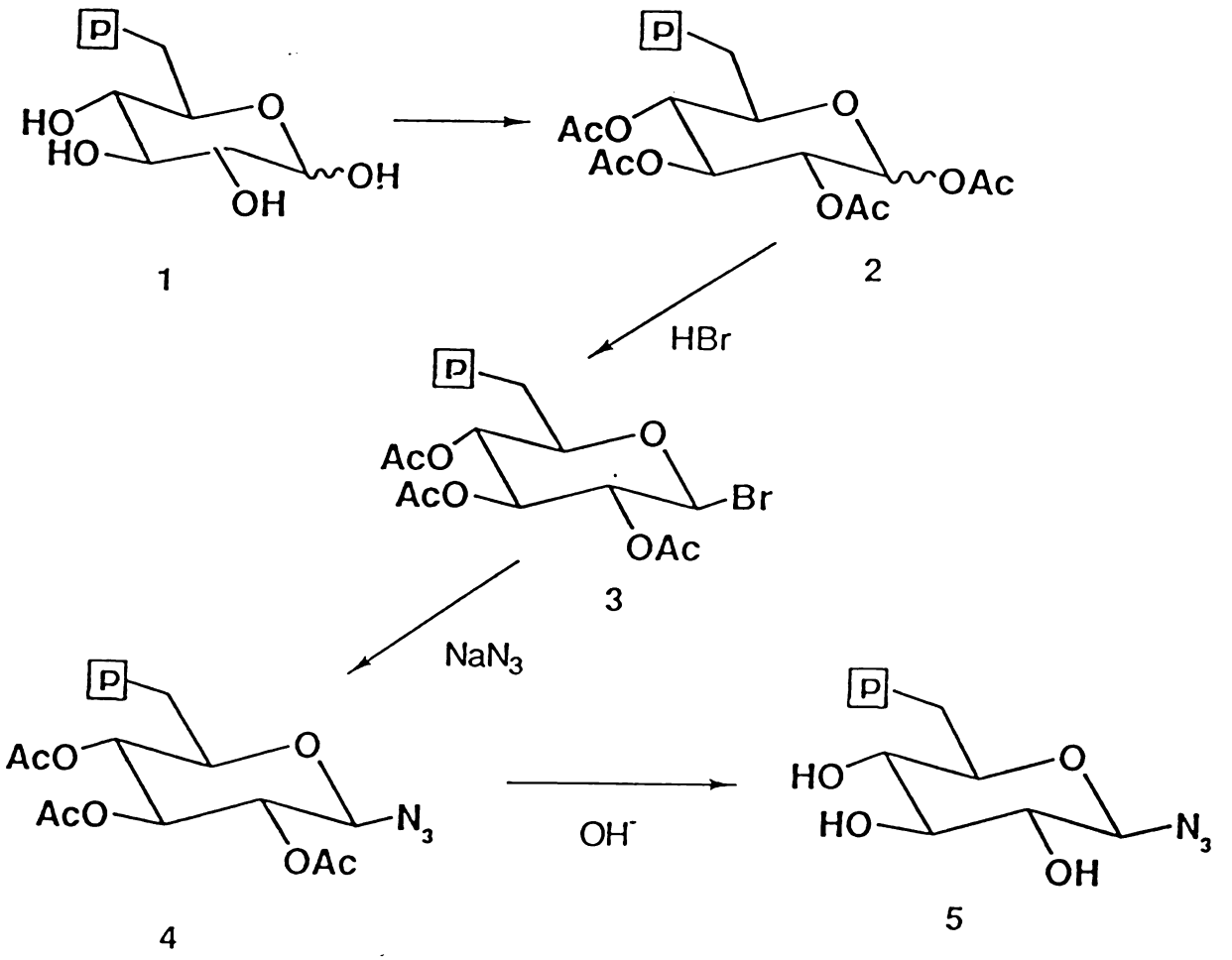

SCHEME 1

48% hydrogen bromide was added with cooling in a -10°C bath and the mixture was then stirred at 10°C for 6 hours. The reaction mixture was concentrated to dryness on a rotary evaporator. The residue **3** was redissolved in 100 ml acetone/methanol (1:1 v/v) and 10 molar equivalents (based on original G6P) of sodium azide and 10 mg t-butyl ammonium bromide was added to the solution. After reflux at 60°C for 16 hours, insoluble material was removed by vacuum filtration and the acetone/methanol were evaporated from the filtrate on a rotary evaporator. The residue containing **4** was redissolved in 15 ml water and pH of the solution was adjusted to 10.5 with 1M NaOH. After 40 minutes, the alkaline mixture was neutralized with formic acid and 1 ml of this solution was then applied to a 1.0 cm (diameter) × 76.5 cm Bio-Gel P2 column equilibrated with 0.1 M ammonium formate, pH 7 (i.e. 0.1 M formic acid titrated with concentrated ammonium hydroxide to pH 7) at a speed of 12ml per hour. After the first 10 ml passed, 23 drop fractions were collected, 42 fractions totally. Based on phosphate assay, there were two partially overlapping phosphate peaks found to be eluted in fraction 24 to 32. The major fractions (24 to 27) of the former peak contained no G6P, while those (28 to 32) of the latter peak contained G6P activity as judged by G6P dehydrogenase assay. Based on conductivity measurement, the other salts eluted after fraction 35. Fractions 24 to 27 were pooled and lyophilized. The

structure of this product **5** was confirmed by ^{1}H-NMR, neg-FAB-mass, and FT-IR.

Synthesis of α,β-D-1-azidoethyl G6P

Scheme 2 outlines synthesis of this compound. 2-Bromoethanol (1 ml) was added to 15 mg G6P (disodium salt) **1**. Then 0.03 ml trifluoroacetic acid was added as acid catalyst. The mixture was stirred at 70°C for 18 hours and then concentrated to dryness *in vacuo* (30°C bath). The residue **6** was dissolved in 8 ml acetone/methanol(1:1 v/v), and 20 mg sodium azide and 1.5 mg t-butyl bromide were added to the solution. After reflux at 60°C for 20 hours, the solvent was evaporated on a rotary evaporator, and the residue was redissolved in 1.5 ml of 0.1M ammonium formate, pH 7. The product was purified using a 1.0 cm (in diameter) × 76.5 cm Bio-Gel P2 column equilibrated with 0.1 M ammonium formate, pH 7, as described earlier. The fractions were then analyzed for organic phosphates and one major phosphate peak at fractions 22 to 26 was pooled and lyophilized. This product **7** gave a single spot positive to orcinol spray after TLC using a isopropanol-1% $(NH_4)_2SO_4$ (2:1 v/v) solvent system. The product **7** had R_f= 0.81 distinct from that of G6P (R_f= 0.43 in the same solvent system). The structure of this product was confirmed by ^{1}H-NMR, neg-FAB-mass, and FT-IR.

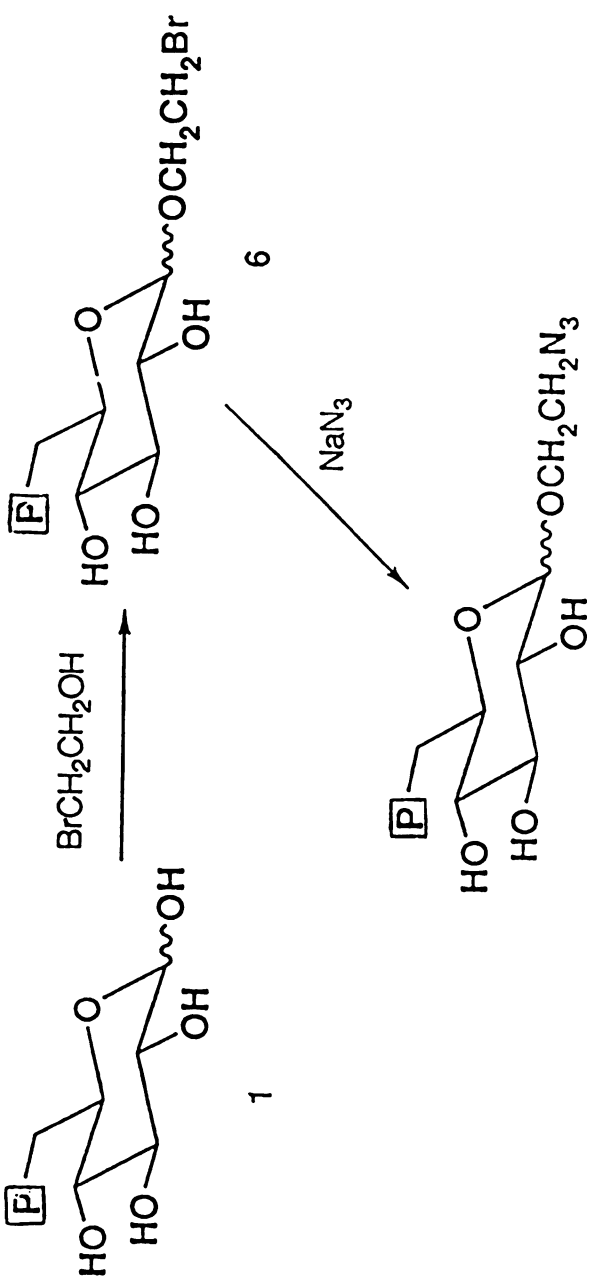

SCHEME 2

Synthesis of β-1-benzyl G6P

Scheme 3 outlines synthesis of this compound. The procedures described by Ness, Fletcher, and Hudson were used in the synthesis of tetrabenzoyl 1-α-D-glucopyranosyl bromide (40). Those described by Helferich and Weis were used in the synthesis of β-D-benzyl glucoside (41). D-glucose **8** (20g) in 240 ml of dry pyridine was heated on the steam bath for 30 minutes and after cooling, 80 ml of benzoyl chloride was added. The reaction flask was heated for one hour at 60°C, 10 ml water was added to the cooled contents and 10 minutes later an additional 100 ml of water, after which the mixture was immediately poured into 2 liters of cold water. There was a cloudy suspension in the flask. The flask was then mildly shaken until white crystals precipitated. The water was removed from the crystals by vacuum filtration. The crystals were further washed with 200 ml fresh water then redissolved in 150 ml chloroform, and this solution was dried with excess anhydrous magnesium sulfate. Chloroform was evaporated by rotary evaporator and the product of β-D-glucose pentabenzoate **9** was obtained. Pentabenzoylated glucose (0.55g) was dissolved in 2 ml dichloroethane and 1 ml glacial acetic acid was added, followed by 3.5 ml of 30% hydrogen bromide in glacial acetic acid. After 2 hours of reaction, the mixture was diluted with 10 ml toluene and then concentrated to a syrup *in vacuo*. The syrup was dissolved in 20 ml dry ether and the

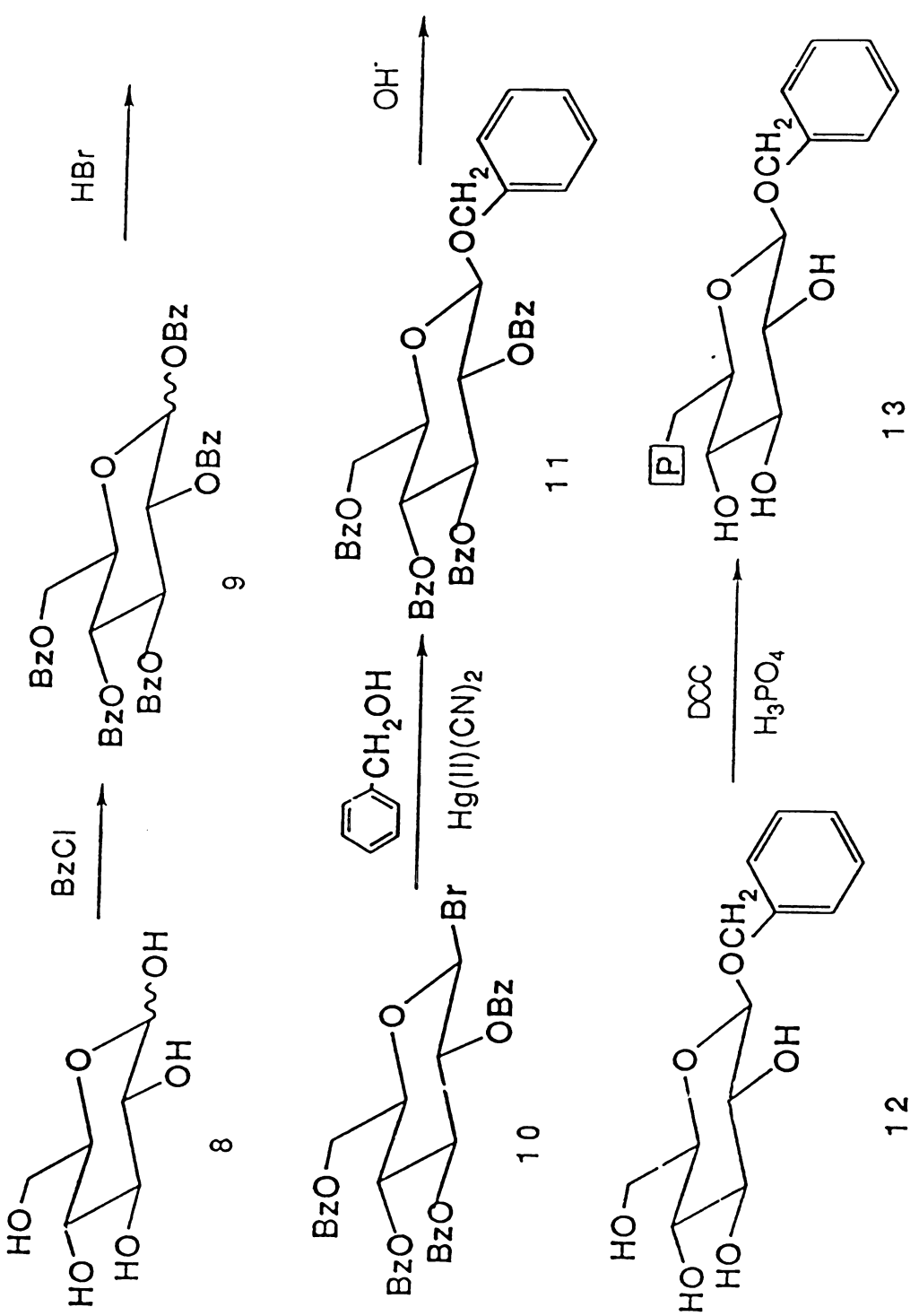

SCHEME 3

ether solution was washed with 20 ml water. The ether was evaporated after drying with anhydrous magnesium sulfate and a sticky crystalline mass containing 2,3,4,6-tetrabenzoyl-α-D-glucopyranosyl bromide **10** was derived. This crystalline mass was dissolved in 5 ml nitromethane and treated with 0.15ml benzyl alcohol and 0.5 g $Hg(II)(CN)_2$ (as a catalyst). After reaction at room temperature for 24 hours, Celite (5 g) was added to the reaction mixture, filtered with a Buchner funnel and the filtrate was then concentrated to dryness. The resulting residue was redissolved in 10 ml toluene and this solution was washed with 2 × 10 ml water. Toluene was evaporated and the residue **11** was redissolved in 25 ml methanol and 20 drops of 1 M NaOH was added for debenzoylation. After 24 hours, methanol was removed on a rotary evaporator and a solution of the residue in 20 ml chloroform was extracted with 2 × 15 ml water. The water layer was then washed with 20 ml chloroform and concentrated to 5 ml. This solution gave two spots positive to orcinol spray after TLC using an ethyl acetate-methanol (4:1 v/v) solvent system, one spot with R_f=0.35 and the other remaining at the origin. The components corresponding to these two different spots were separated by passing 5 ml of the solution through a Pasteur pipet containing 2 ml C18 resin equilibrated with water. The component staying at the origin was eluted with 10 ml water, and then the component with R_f= 0.35 was eluted with 15 ml (7:1 v/v) water-

methanol. The ^{1}H-NMR spectra indicated the product with Rf=0.35 was β-D-benzylglucoside **12**. Then β-D-benzyl glucoside in the eluent above was lyophilized and redissolved in 2 ml dry pyridine. A stock reagent for phosphorylation was prepared by mixing 1 ml 85%(w/w) pyridine with 0.375 g P_2O_5. An aliquot (0.08 ml) of this freshly prepared stock and 0.6 g 1,3-dicyclohexylcarbodiimide (DCC) were added to the solution of β-D-benzylglucoside in pyridine (48). After 48 hours of reaction at room temperature, a very poor yield of one product resulted; this migrated as a single spot positive to orcinol spray after TLC using a isopropanol-1% $(NH_4)_2SO_4$ (2:1v/v) solvent system. Its R_f was slightly smaller than β-D-benzyl glucoside. Pyridine was removed from the reaction mixture <u>in vacuo</u> and 50 ml water was added so that the white solids (dicyclohexylurea resulting from DCC in the reaction) precipitated. The insoluble material was removed by vacuum filtration and the filtrate was concentrated. The phosphorylated product was then purified by P2 column equilibrated with 0.1 M ammonium formate, pH 7.0. Rechromatography of the collected fractions was necessary until the phosphorylated product **13** was well separated from inorganic phosphate. The purity of the product was confirmed by both total and inorganic phosphate assays. The ^{1}H-NMR spectra of this final product was done for structural characterization.

Synthesis of α,β-1-benzyl G6P

Scheme 4 outlines synthesis of this compound. G6P (15 mg, disodium salt) **1** was converted to its TEA salt by passage through an AG 50W-X4(200-400 mesh) column in the triethylammonium form, and the product was lyophilized. The lyophilized white material was redissolved in 1 ml N,N-dimethylformamide, then 3 ml benzyl alcohol and 16 mg p-toluenesulfonic acid were added. The solution was stirred at 60°C for 24 hours. After cooling to room temperature, 6 ml water was added. The two layers were separated and the water layer was washed with 2 × 3 ml toluene. After neutralization with 1N NaOH, the water layer was concentrated to dryness *in vacuo* (55°C bath).The residue was redissolved in 5 ml water. The product was then purified using a Pasteur pipet containing 2 ml C18 resin which had been swollen in methanol and then thoroughly washed with water. The mixture was applied to this C18 column and eluted with water, 10 drop fractions were collected as soon as the mixture was applied. The sugar species in different fractions were identified by orcinol spray after TLC using a isopropanol-1% $(NH_4)_2SO_4$ solvent system. The product **14** with R_f= 0.66 eluted in fraction 11 to 20 and was well separated from G6P with R_f= 0.43 in fraction 5 to 8. Fractions 11 to 20 were then pooled and lyophilized. The structure of the product was confirmed by ^{1}H-NMR and neg-FAB-mass.

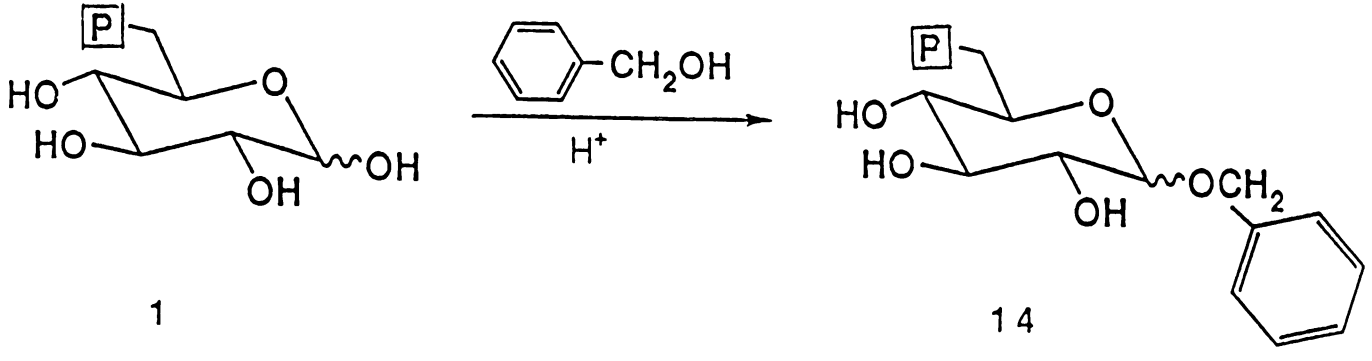

1

14

SCHEME 4

Synthesis of 3-azido-G6P and [^{32}P]-3-azido G6P

Scheme 5 outlines synthesis of this compound. The synthesis of 3-azido-3-deoxy-1,2:5,6-di-O-isopropylidene-α-D-glucofuranose **17** was done as described by Brimacobe et al.(42). 1,2:5,6-di-O-isopropylidene-α-D-allofuranose **15** in 10 ml dry pyridine was treated with 1.5 g p-toluene-sulfonyl chloride in 10 ml dry pyridine, with stirring at room temperature for 38 hours. After 4 ml water was added and stirring continued for another 20 minutes, the mixture was poured into 150 ml ice water. The precipitated white solid was collected by vacuum filtration and redissolved in 200 ml ethanol. The solution was filtered to remove the insoluble material and dried with anhydrous magnesium sulfate. The ethanol was evaporated in vacuo and the shiney white solid product **16** was derived. Then 1.794 g product **16** in 30 ml dimethylformamide was treated with 6 g sodium azide and refluxed at 155-160^0 C for 20 hours. On cooling, 100 ml water was added and the mixture was extracted with 4 × 100 ml chloroform. The organic layer was further washed with 4 × 100 ml water and dried with anhydrous magnesium sulfate. Finally, chloroform and dimethylformamide were removed by evaporation and the residue containing 3-azido-3-deoxy-1,2:5,6-di-O-isopropylidene-α-D-glucofuranose **17** was derived. This residue was redissolved in 2 ml acetonitrile and 4 ml 5 M HCl and 2 ml ethylene glycol were added for hydrolysis (13). This solution was stirred at room

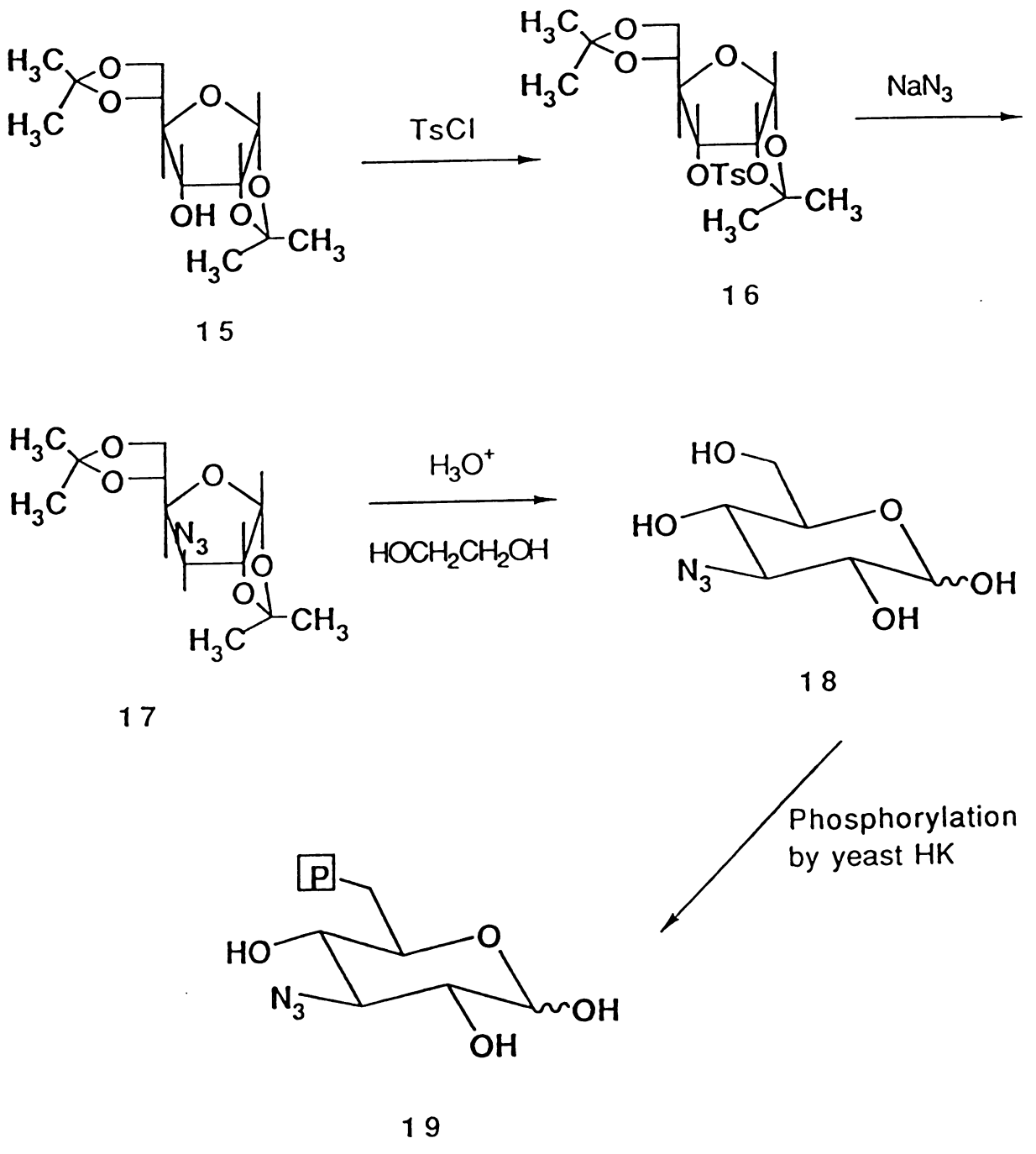

15 16 17 18 19

SCHEME 5

temperature for 24 hours until hydrolysis was complete. Water (30 ml) was then added and the mixture was extracted with 4 × 15 ml chloroform. The water layer was concentrated to a syrup by rotary evaporator (55°C bath) and then diluted with 14 ml water. This solution was saved as the 3-azido-glucose **18** stock, which gave a single spot positive to orcinol spray after TLC using a ethyl acetate-methanol (4:1 v/v) solvent system. The product **18** had a R_f= 0.46 which is distinct from **17** with R_f= 0.76 in the same solvent system. To 7 ml of 3-azido-glucose stock, 1000 units yeast hexokinase, 8ml 220 mM ATP, 0.8 ml 1 M $MgCl_2$ and 1.5 ml 1 M $NaHCO_3$ were added and the total volume was brought up to 34 ml with water. This mixture was incubated at 37°C and the reaction progress was followed by TLC using a isopropanol-1% $(NH_4)_2SO_4$ (2:1 v/v) solvent system. Two distinct spots positive to orcinol spray were detected. One, with R_f= 0.73, corresponded to 3-azido glucose and the other, with Rf= 0.52 was the phosphorylated product **19**. After 24 hours, the phosphorylation was >99% complete and the phosphorylated product was purified by anion-exchange chromatography (43), as follows. 3-Azido-G6P was converted into its acid ester by passage of 5ml aliquots of the phosphorylation mixture through a 1 cm (diameter) × 21.5 cm AG 50W-X4 column (200-400 mesh, hydrogen form, equilibrated with water) and the column was further washed with 10 ml water. The combined effluent was brought up to 30 ml with water. This solution

was adjusted to pH 8.2 with 8.45 M NH_4OH and applied to a 1 cm (diameter) × 26.5 cm AG1-X8 column (200-400 mesh, chloride form, equilibrated in water). The column was first washed with 30 ml 2 mM NH_4OH for removal of the unbound molecules, and then eluted with a salt gradient (linear, 0 to 0.3 M KCl, 120 ml total volume). Forty drop fractions were collected as the gradient started and totally 50 fractions were collected. 3-azido-G6P **19** was shown to be separated from the nucleotides (ATP and ADP) according to the phosphate assay, phenol/H_2SO_4 assay for sugars, and absorbance reading at 260 nm for nucleotides. The fractions containing 3-azido-G6P were pooled and lyophilized and the residue was freed from contaminating salts by Bio-Gel P2 column chromatography as described for β-D-1-azido-G6P. The structure of the product was confirmed by spectroscopic methods including FT-IR, ^{1}H-NMR, and negative-FAB-mass.

The radiolabeled [^{32}P]-3-azido-G6P was prepared as described for the cold compound except that an amount of [γ-^{32}P]-ATP from a 25 Ci/mmole stock was calculated and added to the phosphorylation reaction for a specific activity of 2 mCi/mmole ATP. The purified [^{32}P]-3-azido-G6P had a specific activity of 2 mCi/mmole as it was freshly prepared.

Photolysis of 3-azido-G6P with trypsin-modified native hexokinase

Samples in quartz cuvettes contained trypsin-modified

nativ

azid

The

same

40 c

Depa

mil

fre

Mea

fro

add

add

sam

and

res

tri

aci

sci

cou

SDS-

Wilso

Densi

autora

native hexokinase, the indicated concentration of [^{32}P] 3-azido-G6P and other additions as noted (glucose and G6P). The volume of each different sample was adjusted to be the same with water. The samples were set at a distance of about 40 cm from the xenon chloride laser beam source (Chemistry Department, Michigan State University) and irradiated at 29 milli-watts for the indicated period of time and pulse frequency (i.e. pulses per second).

Measurement of incorporation of [^{32}P] 3-azido-G6P

After various photolysis periods, aliquots were removed from the reaction mixture. Bovine serum albumin (3mg) was added as a carrier and 20% trichloroacetic acid (TCA) was added so that the final concentration of TCA was 5%. The samples were left on ice at least one hour for precipitation and then centrifuged for 2 minutes in a microfuge. The resulting pellet was washed 4 times with 0.2 ml cold 5% trichloroacetic acid and redissolved in 0.3 ml 88% formic acid. This solution was added to 5 ml Safety-Solve scintillant for scintillation spectrometry. Samples were counted in a Beckman LS 9800 Scintillation counter.

SDS-PAGE and autoradiography

SDS-PAGE was performed as described by Polakis and Wilson (10). Gels were stained with Coomassie blue. Densitometric scanning of stained gels (before drying) or autoradiographs was done using Kodak Bio-image densitometer.

RESULTS

Structural characterization of the synthesized G6P analogs

The azido group (N_3) of the covalent azides, RN_3, is characterized by a strong asymmetric stretching band (υ_{as}) near 2100 cm^{-1} and the R group can be considered as a perturbation according to many spectral studies of covalent azides (46). The extensive reports regarding the infrared spectra of organic azides concluded that the asymmetric stretching in the region 2160-2090 cm^{-1} is very strong, only slightly influenced by substituents, and highly characteristic for the azido group (46).

In the synthesis of β-D-1-Azido-G6P (Scheme 1), FT-IR spectrum (Fig. 1) of compound **4** (peracetylated 1-azido-G6P) was obtained. Fig.1 indicated a stretching band occurring at 2116 cm^{-1}, which was consistent with the expected structure of **4**. After the acetyl groups were removed from **4** with mild alkaline hydrolysis, a ^{1}H-NMR spectrum (Fig. 2A) was obtained for the resulting product **5**. The ^{1}H-NMR spectrum of G6P is also given in Fig. 2B to facilitate the assignment of signals in the spectrum of **5**. In solution, G6P exists as a mixture of α and β anomers with different configurations at carbon 1. In Fig. 2B, the two doublet signals at δ 4.6 and δ

Figure 1.

FT-IR spectrum of β-D-1-azido-G6P (peracetylated, i.e. compound **4**)

The spectrum was taken in a Nicolet 710 FT-IR spectrometer using H_2O as a solvent. An asymmetric stretching band centered at 2116 cm^{-1} (as indicated by the arrow) is characteristic for the azido (N_3) group.

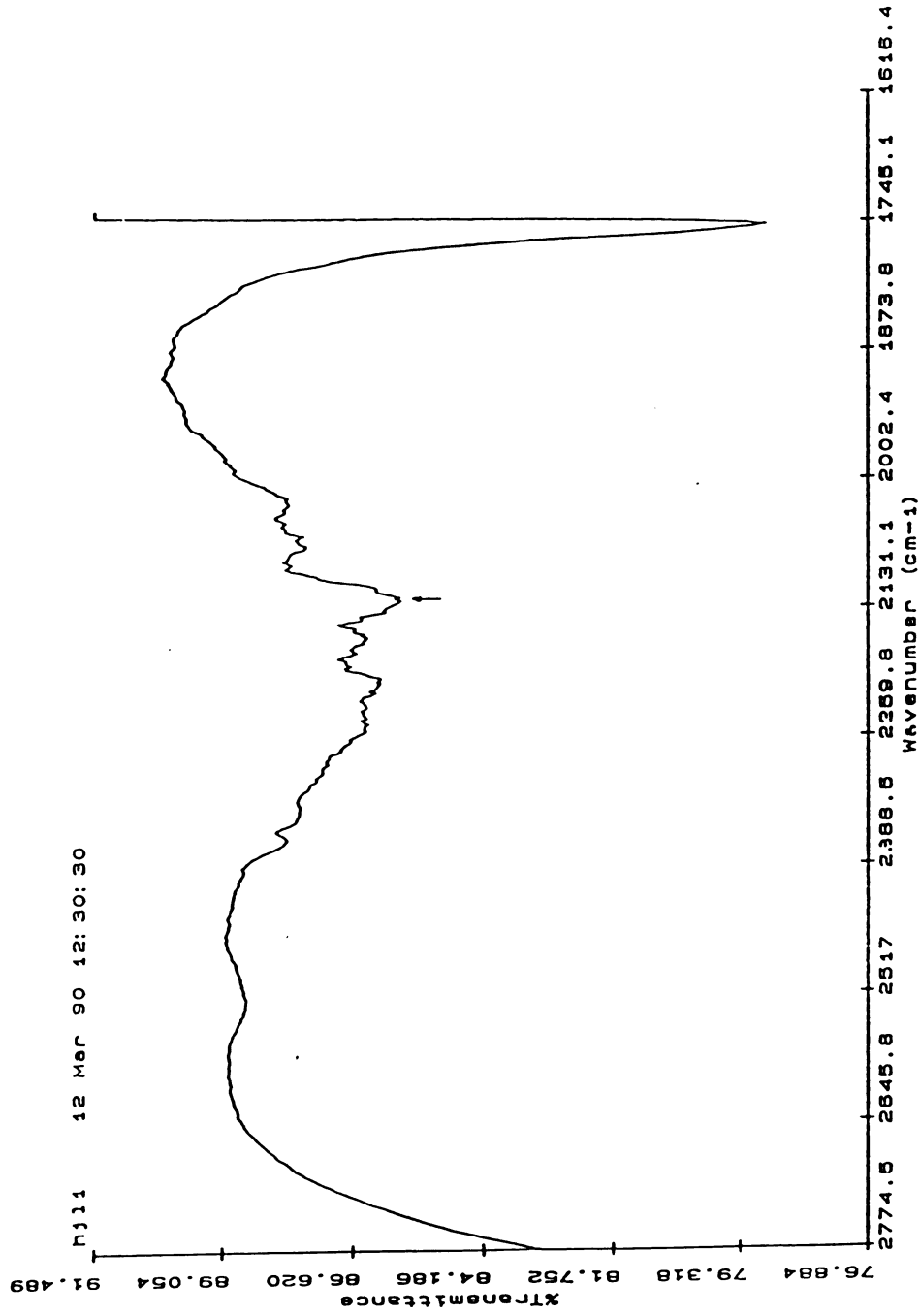
hjll 12 Mar 90 12:30:30
%Transmittance
91.489
89.054
86.620
84.186
81.752
79.318
76.884
2774.5
2645.8
2517
2388.6
2259.8
2131.1
2002.4
1873.8
1745.1
1616.4
Wavenumber (cm-1)

Figure 1

Figure 2.

A. ^{1}H-NMR spectrum of β-D-1-azido-G6P (compound **5**)

B. ^{1}H-NMR spectrum of G6P

Spectrum A was taken in a Bruker 250 MHz spectrometer and Spectrum B in a Varian 300 MHz VXR spectrometer using D_2O as a solvent. The spectrum of G6P in B is shown to facilitate the assignment of the signals in A to the protons of β-D-1-azido-G6P.

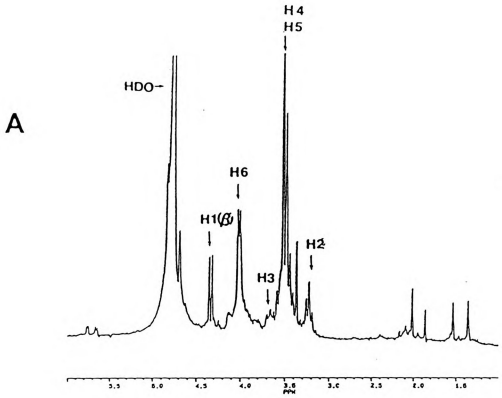

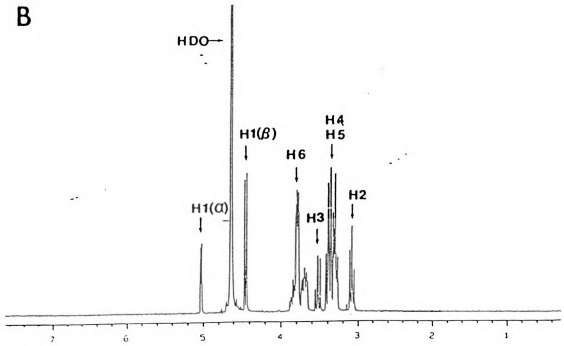

Figure 2

and 5.2 are assigned to protons at carbon 1 of the β and α anomers, respectively. But in Fig. 2A, only the signal at δ 4.3 for H1(β)appears, which indicated only β anomer exists in product **5**. Furthermore, the negative-FAB-mass spectrum of **5** (Fig. 3) gave a major fragment of m/z 273 corresponding to the molecular ion of the monoammonium salt of 1-azido-G6P with the loss of molecular nitrogen (M-H-N_2). Cleophax et al. (49) have prepared various sugar azides and they found no molecular ion of sugar azide, but only peaks corresponding to loss of molecular nitrogen in the mass spectra. Their observation indicated that a loss of molecular nitrogen is common to the sugar azides in mass spectrometry. These spectral data confirmed that the product **5** was β-D-1-azido-G6P.

In the synthesis of α,β-D-1-azidoethyl-G6P (Scheme 2), a mixture of α and β anomers in the product was expected according to the reaction mechanism. The FT-IR spectrum (Fig. 4) was obtained for compound **7** and there was a strong υ_{as} at 2116 cm^{-1} characteristic for N_3 group. Also the neg-FAB-mass spectrum (Fig. 5) of **7** gave a fragment of m/z 328 which corresponded to the acid form of D-1-azidoethyl-G6P (M-H). According to these spectral data, the product **7** was confirmed to be D-1-azidoethyl-G6P.

In the synthesis of β-D-1-benzyl-G6P (Scheme 3), ^{1}H-NMR spectra were obtained for both compound **12** (Fig. 6A) and **13** (Fig. 6B). Both spectra showed the signal at δ 7.2, which

Figure 3.

Negative-FAB-mass spectrum of β-D-1-azido-G6P (compound **5**) The peak with m/e 273 is assigned to the molecular ion of the monoammonium salt of D-1-azido-G6P with the loss of molecular nitrogen ($M-H-N_2$). The peak from the matrix is also indicated.

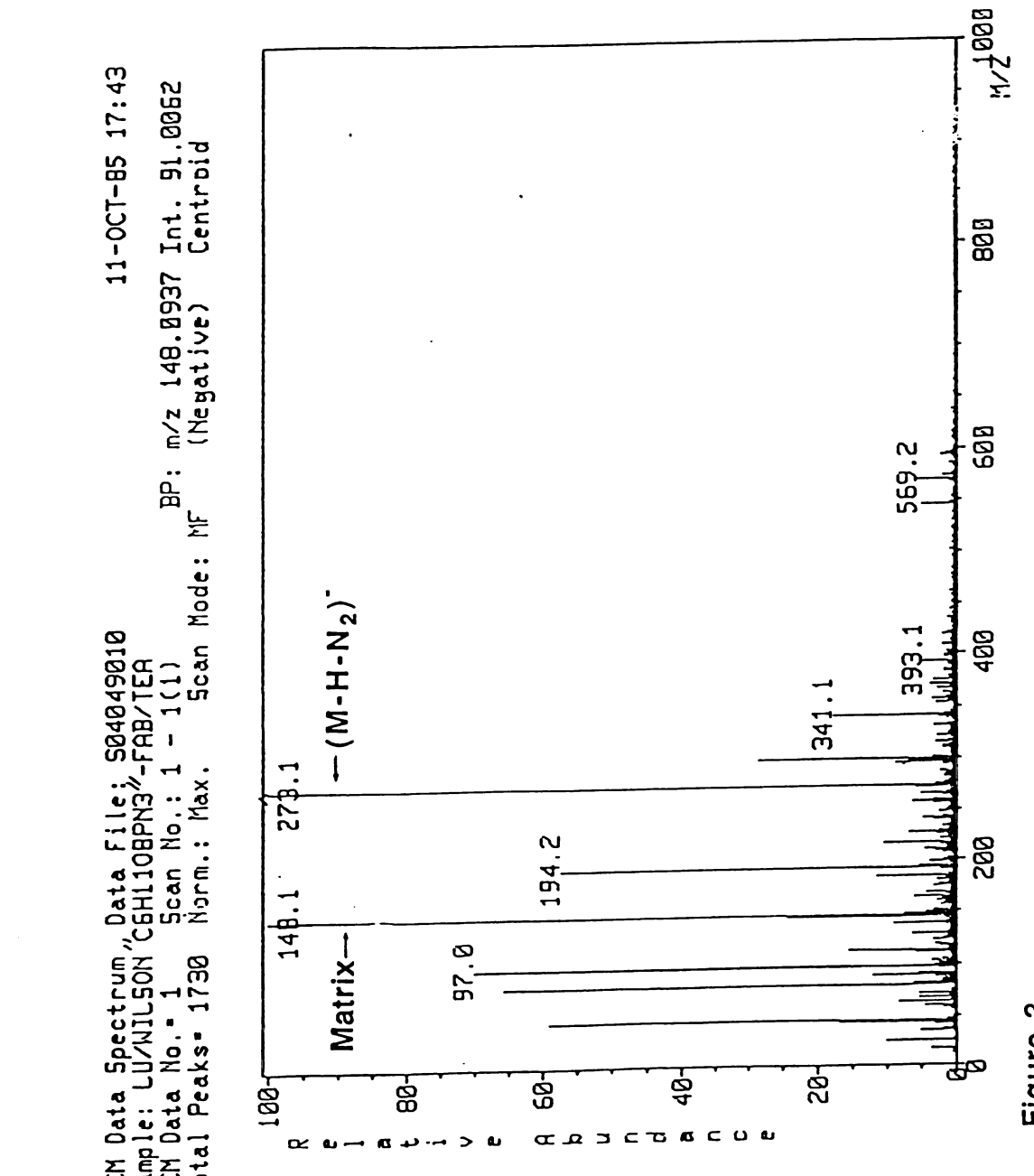
ACM Data Spectrum, Data File; S04049010
Sample: LU/WILSON C6H11OBPN3//-FAB/TEA
ACM Data No.= 1 Scan No.: 1 - 1(1)
Total Peaks= 1730 Norm.: Max. Scan Mode: MF
11-OCT-85 17:43
BP: m/z 148.0937 Int. 91.0062
(Negative) Centroid
Relative Abundance
Matrix
148.1
273.1
-(M-H-N2)-
97.0
194.2
341.1
393.1
569.2
m/z

Figure 3

Figure 4.

FT-IR spectrum of D-1-azidoethyl-G6P (compound 7)

This spectrum was taken in a Nicolet 710 FT-IR spectrometer using H_2O as a solvent. A strong asymmetric stretching band centered at 2116 cm-1 is characteristic for the azido group.

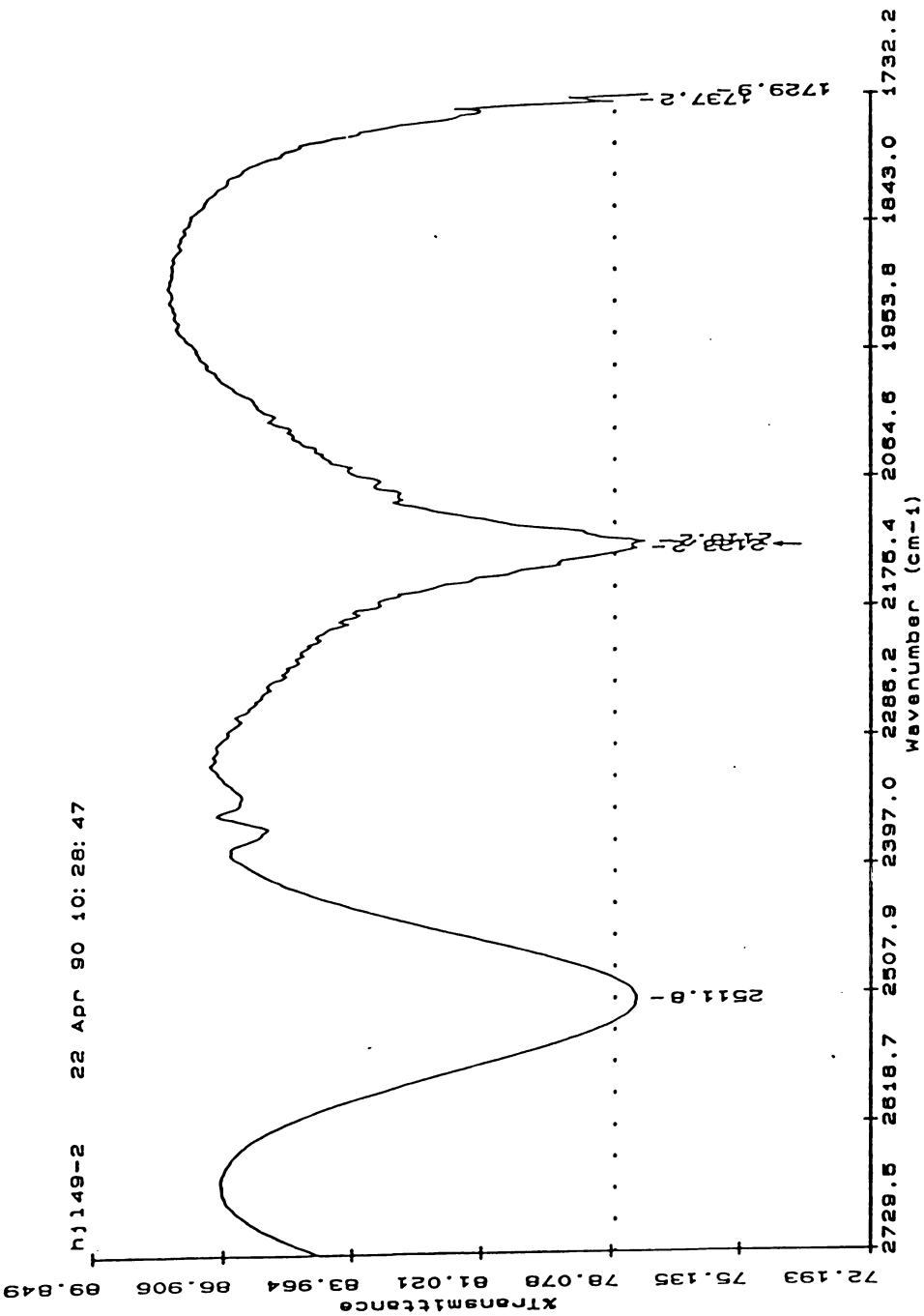
h1149-2
22 Apr 90 10:28:47
Transmittance
72.193
75.135
78.078
81.021
83.964
86.906
89.849
2728.5
2618.7
2507.9
2397.0
2288.2
2175.4
2064.6
1953.8
1843.0
1732.2
Wavenumber (cm-1)
2511.8
2210.2
1729.2

Figure 4

Figure 5.

Negative-FAB-mass spectrum of D-1-azidoethyl-G6P (compound 7)

The molecular ion with m/e 328 of 1-azido-ethyl-G6P is indicated by $(M-H)^-$.

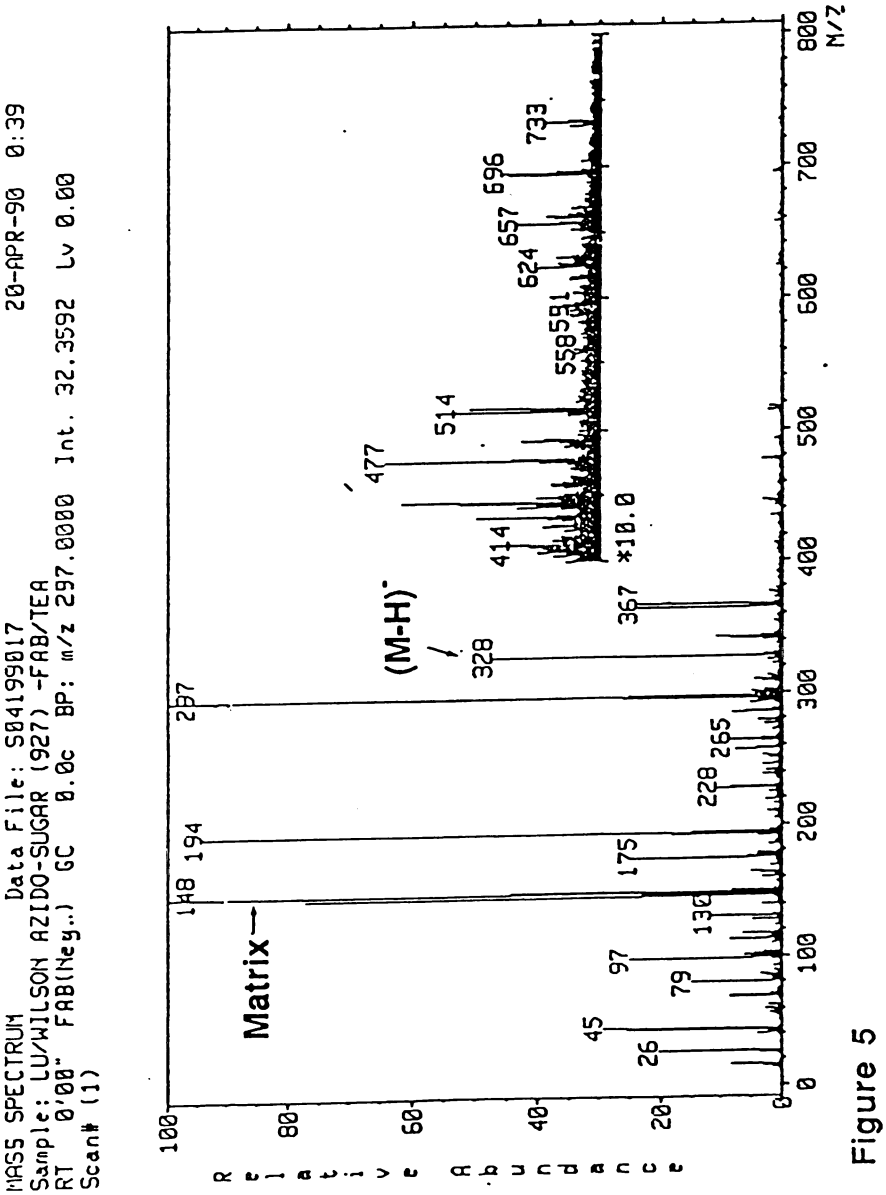
MASS SPECTRUM Data File: S04199017
Sample: LU/WILSON AZIDO-SUGAR (927) -FAB/TEA
RT 0'00" FAB(Neg..) GC 0.0c BP: m/z 297.0000 Int. 32.3592 Lv 0.00
Scan# (1)
20-APR-90 0:39
Matrix
(M-H)⁻
*10.0
Relative Abundance
M/Z

Figure 5

Figure 6.

A. ^{1}H-NMR spectrum of β-D-1-benzyl-glucose (compound **12**)

B. ^{1}H-NMR spectrum of β-D-1-benzyl-G6P (compound **13**)

The spectra were taken in a Varian 300 MHz VXR spectrometer using D_2O as a solvent. Both spectra showed a doublet signal for the β-anomeric proton but none for the α-anomeric proton, which indicated there were only β anomers in compound **12** and **13**.

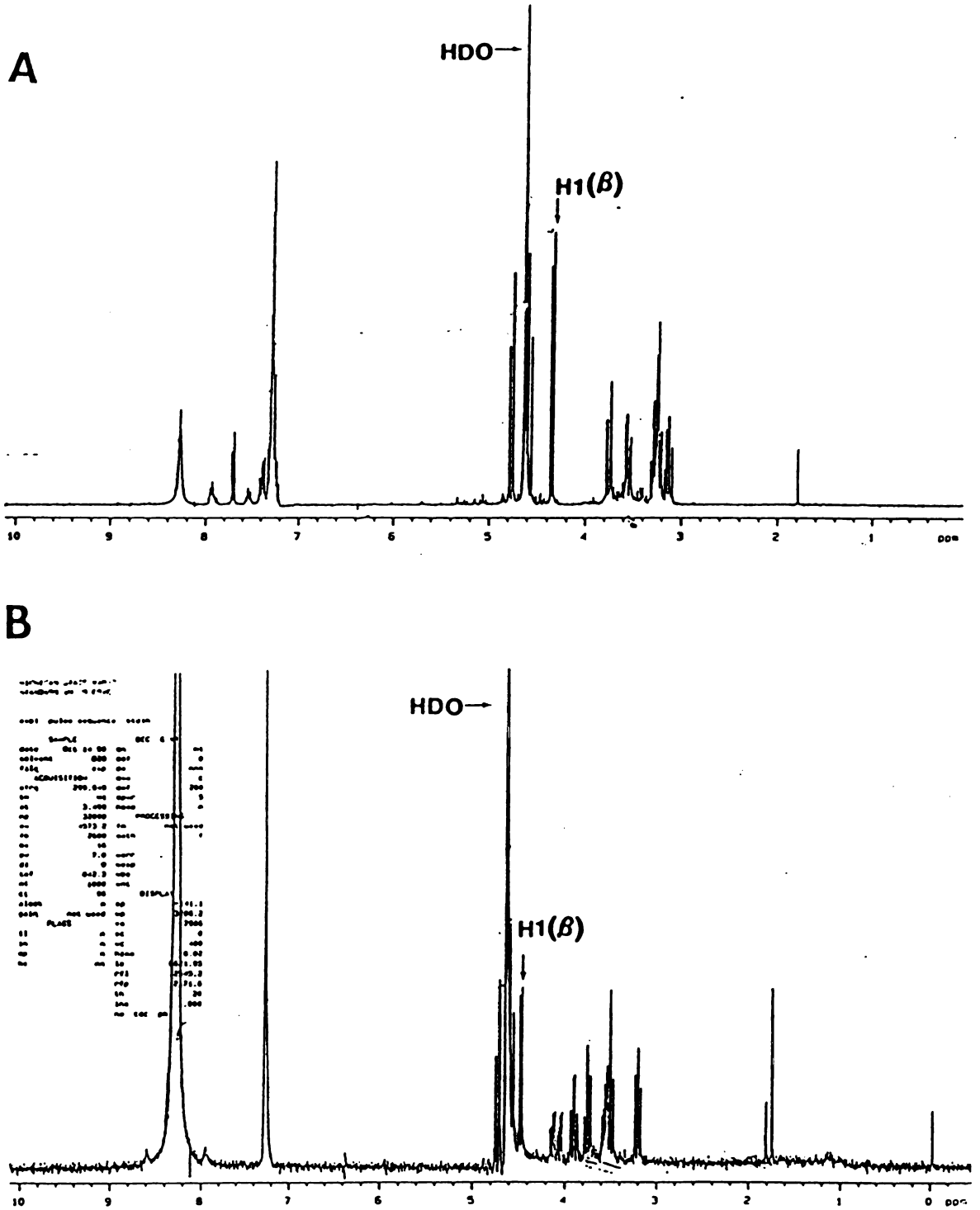

Figure 6

was assigned to the protons directly attached to the benzene ring. The peaks at 4.5-4.7 ppm bracketing the water peak at 4.6 ppm were assigned to the protons on $-CH_2-$ of the benzyl group. Also, similar to compound **5**, a doublet at δ 4.4 but not at the more downfield position (about δ 5.2 for H1 in α form), indicated that **12** and **13** were β anomers.

In the synthesis of α,β-D-1-benzyl-G6P (Scheme 4), ^{1}H-NMR spectrum of **14** (Fig. 7) was similar to that of **13**. However the spectrum showed the doublet signals of H-1 at δ 5.2 (for H_α) and δ 4.4 (for H_β) which indicated a mixture of α and β anomers. Based on a visual comparison of areas of the two doublet signals for α and β anomeric protons, the product was estimated to contain 70-80% of α anomer.

In the synthesis of 3-azido-G6P (Scheme 5), the structures of compounds involved were characterized either spectroscopically or enzymatically. An FT-IR spectrum was obtained for compound **17** (Fig. 8). Fig 8 indicated a strong asymmetric stretching band at 2123 cm^{-1} which was characteristic for N_3. The isopropylidine groups were removed from **17** to yield **18**. Compound **18** was a substrate of yeast hexokinase, and was transformed to compound **19** by enzymatic phosphorylation. Compound **19** was found to be a substrate (K_m = 1 mM) of G6P dehydrogenase, which indicated the structural resemblance of **19** to G6P. Furthermore, the neg-FAB-mass spectrum of **19** (Fig. 9) gave a fragment of m/z 284 corresponding to the acid form of 3-azido-G6P. Based on

Figure 7.

^{1}H-NMR spectrum of α,β-D-1-benzyl-G6P (compound **14**, a TEA salt)

This spectrum was taken in a Varian 300 MHz VXR spectrometer using D_2O as a solvent. The doublet signals for both α and β anomeric protons are indicated. Part of the identical spectrum, with an expanded scale, was shown at the bottom for comparing areas of the signals for α and β anomeric protons.

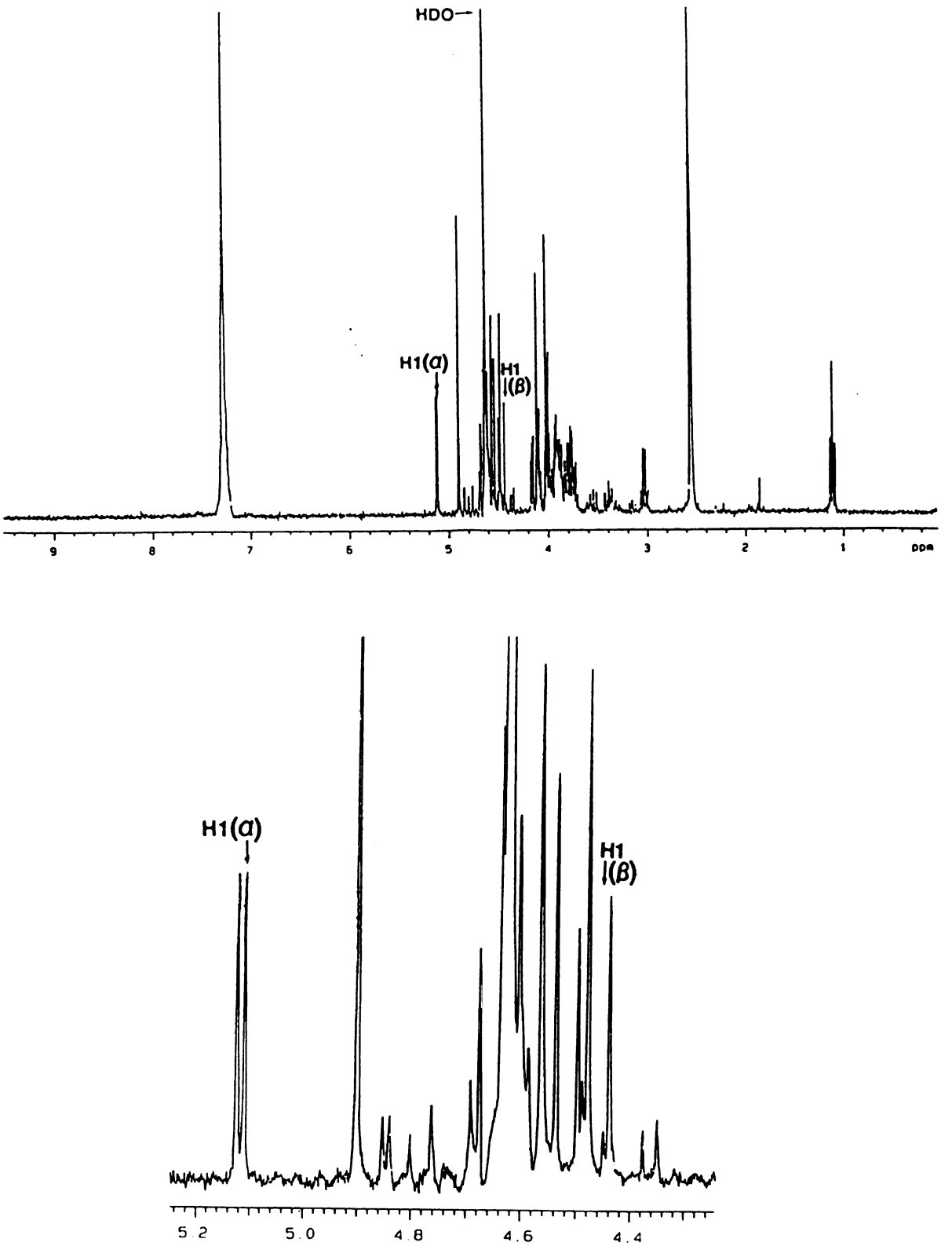

Figure 7

Figure 8.

FT-IR spectrum of 3-azido-1,2:5,6 di-O-isopropylidine-D-glucofuranose (compound **17**)

A strong asymmetric stretching band centered at 2123 cm^{-1} is characteristic for the azido group.

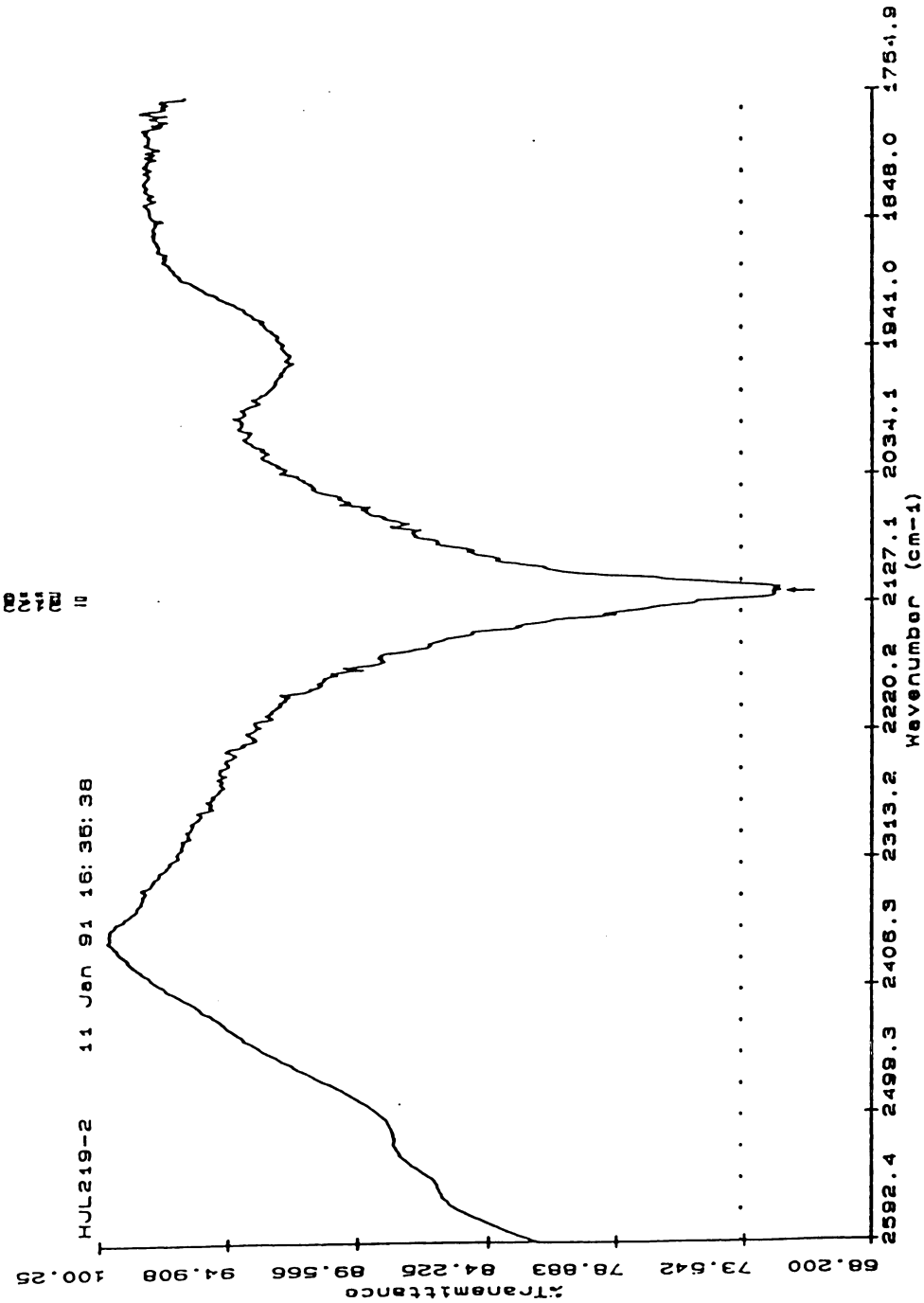
HJL219-2
11 Jan 91 16:36:38
%Transmittance
100.25
94.908
89.566
84.225
78.883
73.542
68.200
2592.4
2499.3
2406.3
2313.2
2220.2
2127.1
2034.1
1941.0
1848.0
1754.9
Wavenumber (cm-1)

Figure 8

Figure 9.

Negative-FAB-mass spectrum of 3-azido-G6P (compound **19**)

The molecular ion with m/e 284 is indicated by $(M-H)^-$.

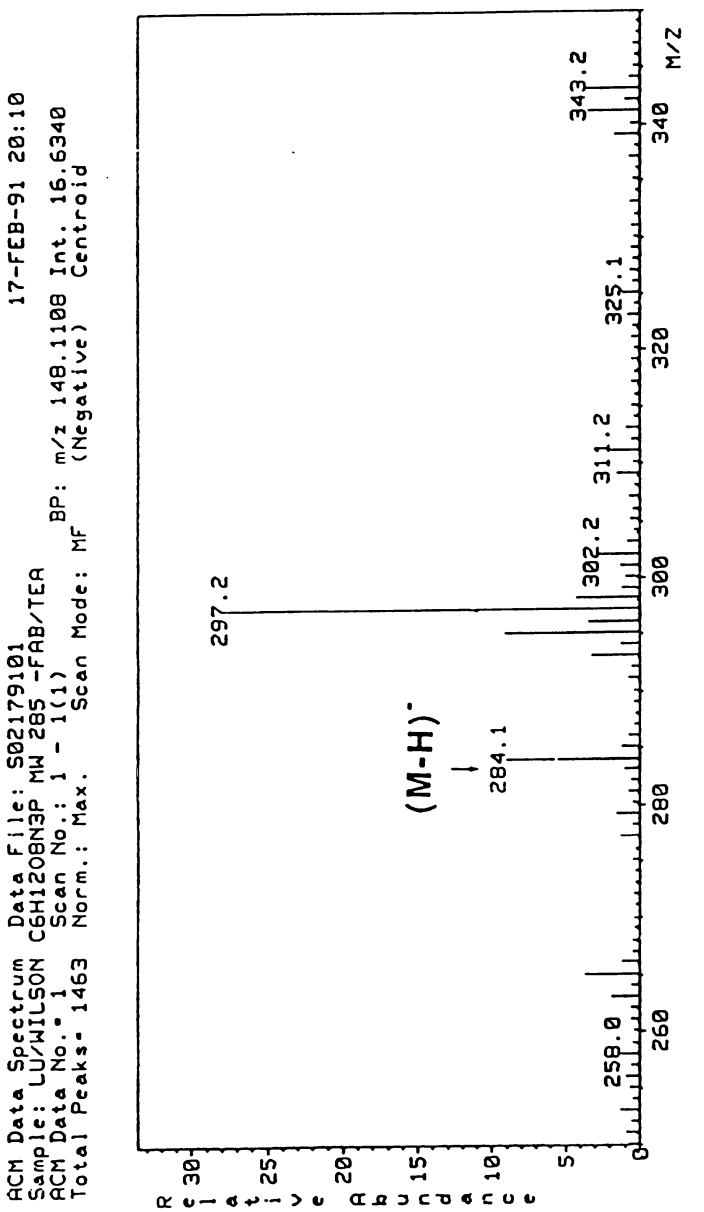
ACM Data Spectrum Data File: S02179101
Sample: LU/WILSON C6H12O8N3P MW 285 -FAB/TEA
ACM Data No.: 1 Scan No.: 1 - 1(1)
Total Peaks= 1463 Norm.: Max. Scan Mode: MF
17-FEB-91 20:10
BP: m/z 148.1108 Int. 16.6340
(Negative) Centroid
Relative Abundance
M/Z
(M-H)⁻
258.0
284.1
297.2
302.2
311.2
325.1
343.2

Figure 9

the spectroscopic and enzymatic characterizations, compound 19 was confirmed to be 3-azido-G6P.

Kinetic studies on the inhibitory effectiveness of the synthesized G6P analogs

The inhibitory effectiveness of these G6P analogs on brain hexokinase activity was evaluated by kinetic studies. The results indicated that modifications at C-1 or C-3 of G6P resulted in decreased inhibitory effectiveness.

Based on Lineweaver-Burk plots of the inhibition kinetics, α,β-D-1-azidoethyl-G6P (Fig. 10), α,β-1-benzyl-G6P (Fig. 11) and 3-azido-G6P (Fig. 12) were shown to be competitive versus substrate ATP as G6P was (1). Using the EZ-fit program described in Methods, the K_m values of the substrates and the K_i values of inhibitors were derived. The K_m values for ATP varied somewhat, but were in the range of 0.5 to 0.7 mM. α,β-D-1-Azidoethyl-G6P had a K_i= 0.03 mM which was comparable to that of G6P (K_i= 0.026 mM) (50). α,β-D-1-benzyl-G6P containing 70-80% of α anomers had a K_i= 0.23 mM which was about 8 times higher than that of G6P. 3-azido-G6P was a very poor competitive (vs ATP) inhibitor (K_i= 2.6 mM) which was 100 fold less potent than G6P.

The inhibition of hexokinase activity with either β-D-1-azido-G6P or β-D-1-benzyl-G6P were not detectable at concentrations of 1.66 mM and 1 mM, respectively, with ATP

Figure 10.

Inhibition of rat brain hexokinase by α,β-D-1-azidoethyl-G6P

Hexokinase activity was determined using the glucose-6-phosphate assay as described in Methods.

K_m = 0.54 mM

K_i = 0.03 mM

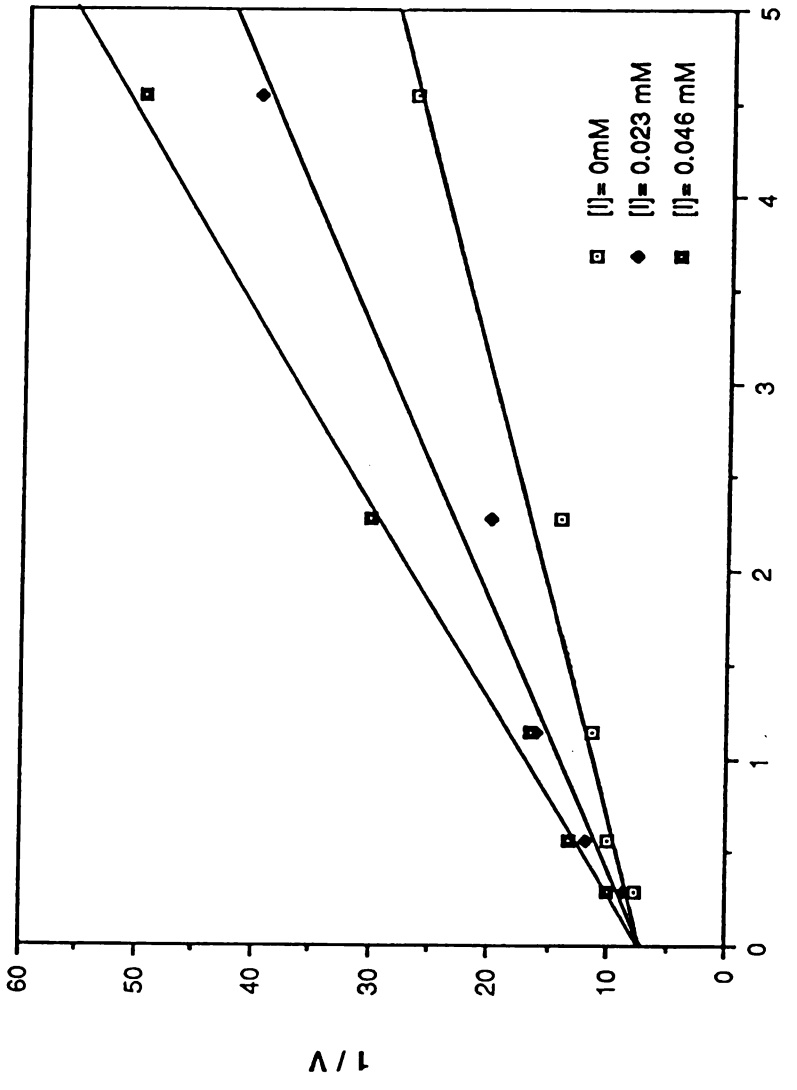

Figure 10

Figure 11.

Inhibition of rat brain hexokinase by α,β-D-1-benzyl-G6P. Hexokinase activity was determined using the glucose-6-phosphate assay as described in Methods.

K_m = 0.68 mM

K_i = 0.23 mM

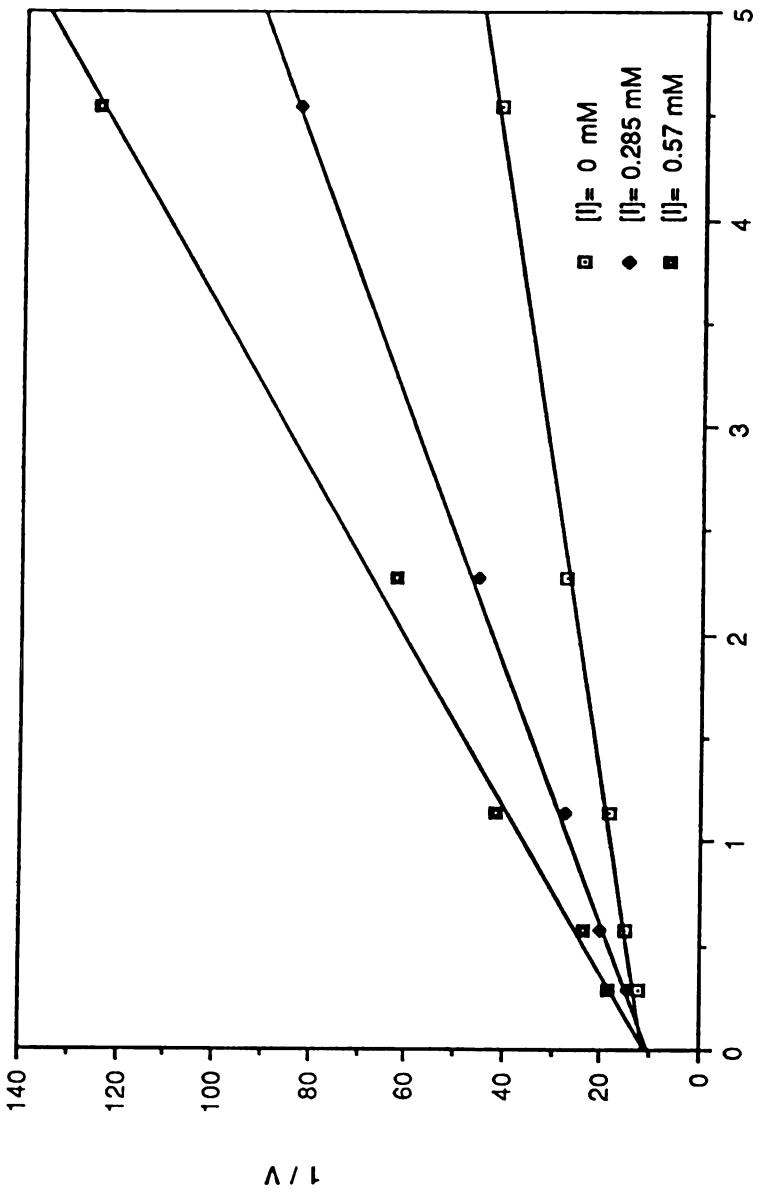

Figure 11

Figure 12.

Inhibition of rat brain hexokinase by 3-azido-G6P. Hexokinase activity was determined using the pyruvate kinase-lactate dehydrogenase coupled assay as described in Methods.

K_m = 0.50 mM

K_i = 2.60 mM

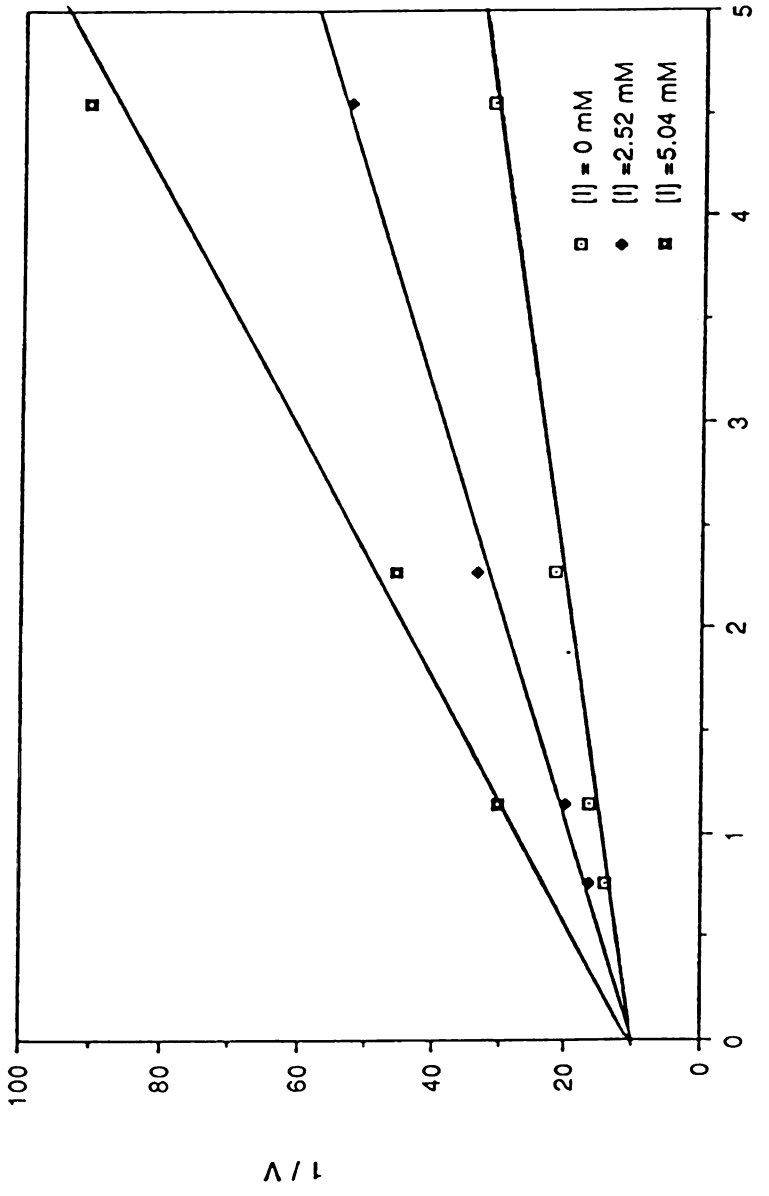

Figure 12

concentration of 1.76 mM. With the assumption that an inhibition of 5% would have been detected, we can estimate the minimum K_i values for these compounds. Therefore, if β-D-1-azido-G6P and β-D-1-benzyl-G6P were competitive inhibitors of hexokinase, they must have their K_i values at least a thousand times higher than that of G6P.

The apparent K_i values derived for these synthesized G6P analogs were summarized in Table II for comparison.

The ultraviolet spectrum of 1-azidoethyl-G6P and an unsuccessful attempt to use this derivative in photoaffinity labeling of hexokinase

The ultraviolet spectrum of 1-azidoethyl-G6P (not shown) exhibited a strong absorption band near 200 nm, but no absorption above 300 nm.

Irradiation with a high-pressure mercury lamp having emission wavelengths in the lower 200 nm range failed to produce measurable incorporation of [^{14}-C] 1-azidoethyl-G6P into hexokinase.

Unsuccessful attempts to synthesize α-1-azidobenzyl-G6P

Since aryl azides were reported to be more applicable than alkyl azides in photolabeling of macromolecules, α-1-azidobenzyl-G6P was of interest as a photoactivatable ligand for labeling the G6P binding site of brain hexokinase. Two different synthetic routes were tried; however, neither 2-

TABLE II

EFFECTS OF G6P AND THE SYNTHESIZED ANALOGS ON BRAIN HEXOKINASE ACTIVITY

Modification at carbon No.	Compound	K_i (mM)
0	G6P	0.026[a]
1	β-D-1-azido-G6P	> 10[b]
1	α,β-D-1-azidoethyl-G6P	0.03
1	β-D-1-benzyl-G6P	> 20[b]
1	α,β-D-1-benzyl-G6P	0.23
3	D-3-azido-G6P	2.6

[a] This K_i value of G6P was quoted from Grossbard et al. (50).

[b] The K_i values were estimated with the assumption 5% inhibition would have been detected with [ATP]= 0.5 mM and [I]= 1 mM and 1.66 mM for β-D-1-azido-G6P and β-D-1-benzyl-G6P, respectively.

azidobenzyl alcohol nor 2-nitrobenzyl alcohol reacted with G6P under conditions similar to the synthesis of α,β-1-benzyl-G6P. Therefore, possible photoaffinity labeling of the G6P-binding site on brain hexokinase with an aryl azide was not further pursued.

The ultraviolet spectrum of 3-azido-G6P and the choice of suitable light source for photoaffinity labeling of hexokinase

The ultraviolet spectrum of 3-azido-G6P (Fig. 13) showed a strong absorption band at about 200 nm and a fairly weak band centered at about 300 nm.

The UV lamps and flash apparatus, which have been used in photolysis of many aryl azide compounds for crosslinking or affinity labeling purposes, failed to give measurable incorporation of [^{32}P]3-azido-G6P into hexokinase after 6 hours of irradiation. Also, prolonged irradiation caused protein degradation as judged by the appearance of multiple fragments after SDS-polyacrylamide gel electrophoresis. However, the xenon chloride laser at 308 nm was successfully used as a good energy source for efficient generation of radical species from 3-azido-G6P with avoidance of protein degradation during photolysis.

Figure 13.

The ultraviolet spectrum of 3-azido-G6P

In this spectrum, there was a strong absorption band at about 200 nm and a weak band centered at about 300 nm as indicated by the arrows. These two bands are characteristic for the alkyl azides as described by Closson and Gray (54).

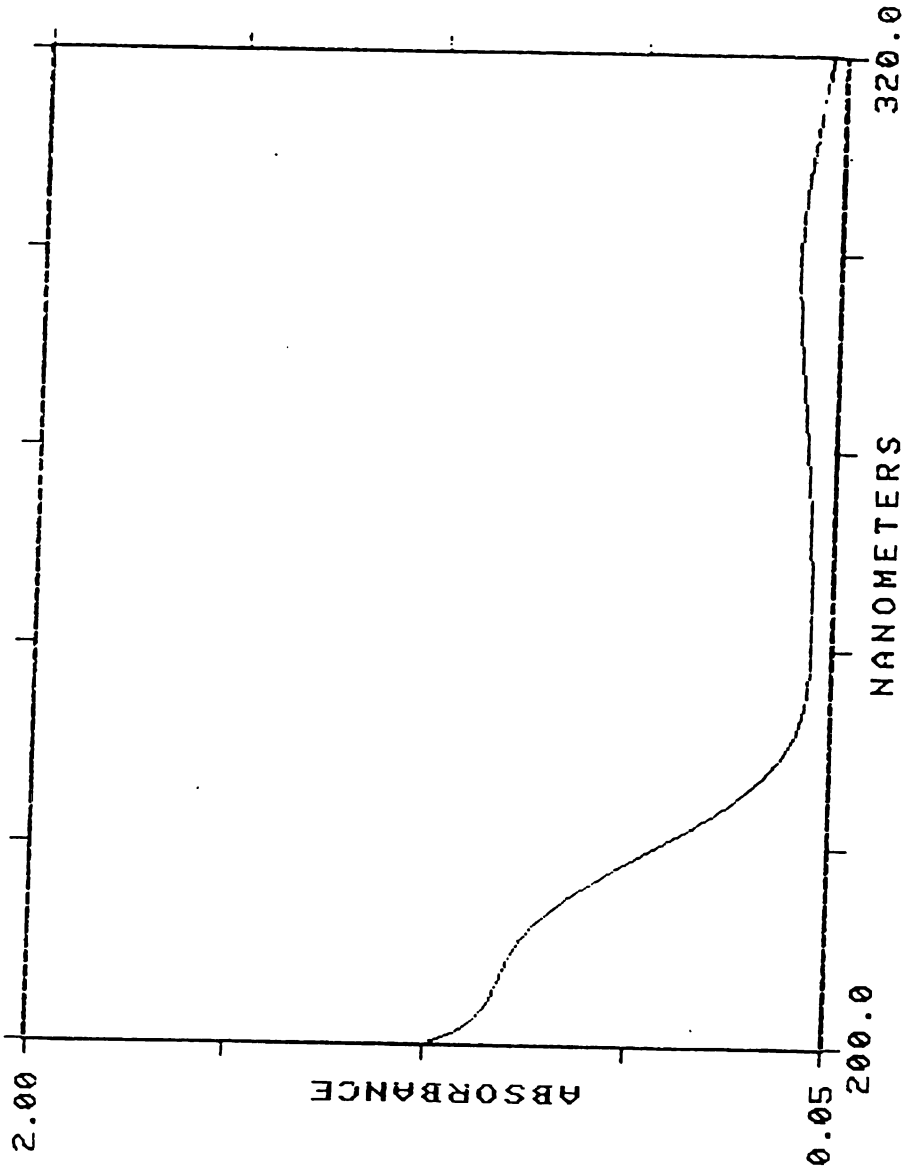

Figure 13

The effect of irradiation on trypsin-modified hexokinase activity

The trypsin-modified hexokinase activity was measured before and after irradiation. The retention of activity varied from one experiment to another, but it remained in the 70% to 80% range after irradiation at 50 Hz for 5 minutes or 25 Hz for 10 minutes.

Labeling of trypsin-modified native hexokinase with 3-azido-G6P

As the 3-azido-G6P labeled hexokinase was far more susceptible to proteolysis by trypsin, it gave many other digestion fragments beside the major ones. These fragments made the result from SDS gel electrophoresis complicated and the autoradiogram very difficult to interpret.

However, it has previously been demonstrated (10) that the 10, 40, 50 kDa fragments resulting from tryptic cleavage of hexokinase remain associated *via* noncovalent interactions, with retention of catalytic activity and little change in the kinetic parameters (i.e. K_m, K_i) for glucose, ATP and G6P, and with retention of the ability to associate in a G6P-sensitive manner with the outer mitochondrial membrane. Thus it was used in these photoaffinity labeling experiments so that the problem described above could be avoided.

The trypsin-modified hexokinase (0.3 mg/ml), after

incubation with 6 mM glucose, 5 mM 3-azido-G6P (about 2 times its K_i) and other ligands (as noted in Fig. 14), was irradiated by a xenon chloride laser beam at either 25 Hz for 10 minutes or 50 Hz for 5 minutes. All the proteolyzed fragments were radiolabeled based on the SDS polyacrylamide gel electrophoresis and autoradiography (Fig. 14). Densitometric quantitation of these bands on both the Coomassie blue stained gel (before drying) and its corresponding autoradiogram indicated the 50 kDa fragment was labeled at more than twice the density of labeling of other fragments (Table III). The 10 kDa fragment was ignored in these comparisons since the darker background near the bottom of the autoradiogram precluded accurate quantitation. Also, irradiation at either 50 Hz for 5 minutes or 25 Hz for 10 minutes resulted in the same extent of labeling, as expected because the quantum yield of nitrenes from 3-azido-G6P should be a constant and the total amount of photons irradiated on each sample was equal in both conditions.

If the dense labeling of the 50 kDa fragment were due to the specific recognition of the hexokinase regulatory site (G6P binding site) by 3-azido-G6P, the addition of G6P should antagonize the 3-azido-G6P binding and thus prevent labeling. However, contrary to what was expected, the addition of 10 mM G6P (1000 times the K_i value) did not eliminate the labeling at the 50 kDa fragment (Table III).

Figure 14.

The Coomassie blue stained gel and its autoradiograph of the [^{32}P] 3-azido-G6P labeled hexokinase (trypsin-modified) The trypsin-modified hexokinase (0.3 mg/ml) was incubated with 6 mM glucose, 5 mM [^{32}P] 3-azido-G6P, and with or without 10 mM G6P as indicated. Also, samples were irradiated at 25 Hz for 10 minutes or 50 Hz for 5 minutes by xenon chloride laser as indicated below. A.(top) is the Coomassie blue stained gel, and B.(below) is the corresponding autoradiograph of A. Lane 1: no G6P; 25 Hz for 10 min., lane 2: 10 mM G6P; 25 Hz for 10 min., lane 3: no G6P; 50 Hz for 5 min., lane 4: 10 mM G6P; 50 Hz for 5 min.

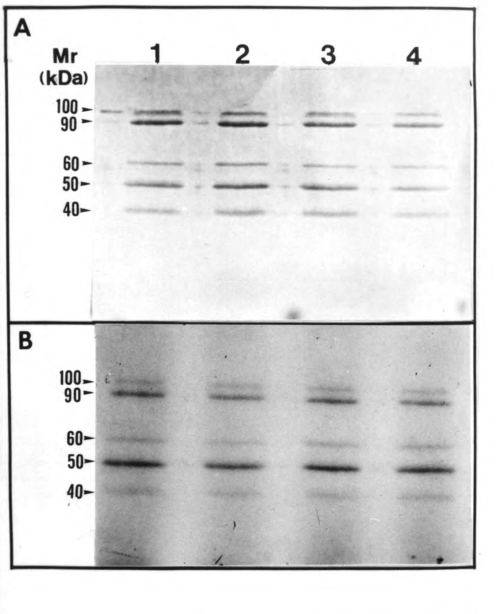

Figure 14

TABLE III

RELATIVE SPECIFIC ACTIVITY OF LABELING ON TRYPSIN-MODIFIED BRAIN HEXOKINASE FRAGMENTS

Irradiation condition	Relative Specific Activity[a]			
	25 Hz; 10 min		50 Hz; 5 min	
	10 mM	No G6P	10 mM G6P	No G6P
40 kDa	0.72	0.62	0.85	0.78
50 kDa	1.79	1.93	1.93	2.05
60 kDa	0.86	0.78	0.74	0.61
90 kDa	0.78	0.84	0.82	0.81
100 kDa	0.52	0.61	0.50	0.50

[a] Trypsin modified native hexokinase (0.3 mg/ml) was incubated with [^{32}P] 3-azido-G6P (5 mM, about 1.75 mC$_i$/mmole) and with or without G6P (10 mM) as indicated, then irradiated by XeCl laser at either 25 Hz for 10 minutes or 50 Hz for 5 minutes. The fragments of brain hexokinase in the irradiated samples were separated by SDS-PAGE. Densitometric quantitation of the bands on both the Coomassie blue stained gel and its corresponding autoradiogram gave the relative intensity of each band.

$$\text{Relative specific activity} = \frac{\text{Relative intensity on autoradiograph}}{\text{Relative intensity on Coomassie blue gel}}$$

which reflects the density of radioactivity incorporated to each protein fragment.

Time course of [^{32}P]3-azido-G6P incorporation

Measurement of incorporation of [^{32}P]-3-azido-G6P into hexokinase molecules during the irradiation period was performed as described in Methods and the progress curves were derived (Fig. 15). Irradiated samples with and without G6P were compared. The curves showed that incorporation of 3-azido-G6P into hexokinase increased with the irradiation time, with maximal incorporation after approximately 15 minutes. But the difference of incorporation between the samples with and without G6P was small; about 25% difference was found at the time point where the incorporation was maximal.

After 20 minutes of irradiation, 3-azido-G6P in the sample was not completely photolyzed, as judged by TLC, so that cessation of further incorporation was not due to a depletion of the reagent. Alternatively, another possibility was that if there were only one specific G6P binding site in hexokinase and 3-azido-G6P binds at that site, then incorporation of radioactivity would cease when that site was fully labeled. However, it was also expected that competition with a large excess (10 mM) of G6P should decrease labeling. But, in Fig.15, only modest protection of brain hexokinase against labeling with 3-azido-G6P was seen when G6P (10 mM) was added. Therefore, we do not have the explanation for this phenomenon.

Figure 15.

Time course of [^{32}P] 3-azido-G6P incorporation to brain hexokinase

The trypsin-modified hexokinase (0.3 mg/ml) was incubated with 6 mM glucose, 5 mM [^{32}P] 3-azido-G6P with the specificity 0.43 mCi/mmole, and either with or without 10 mM G6P. The mixtures were irradiated by xenon chloride laser at 25 Hz for 0-20 minutes. Aliquots were removed from the reaction mixture after various photolysis periods for measuring the incorporation of [^{32}P] 3-azido-G6P to hexokinase as described in Methods. G6P in the mixture did not show significant protection of hexokinase from labeling according to a comparison of the two curves in this figure.

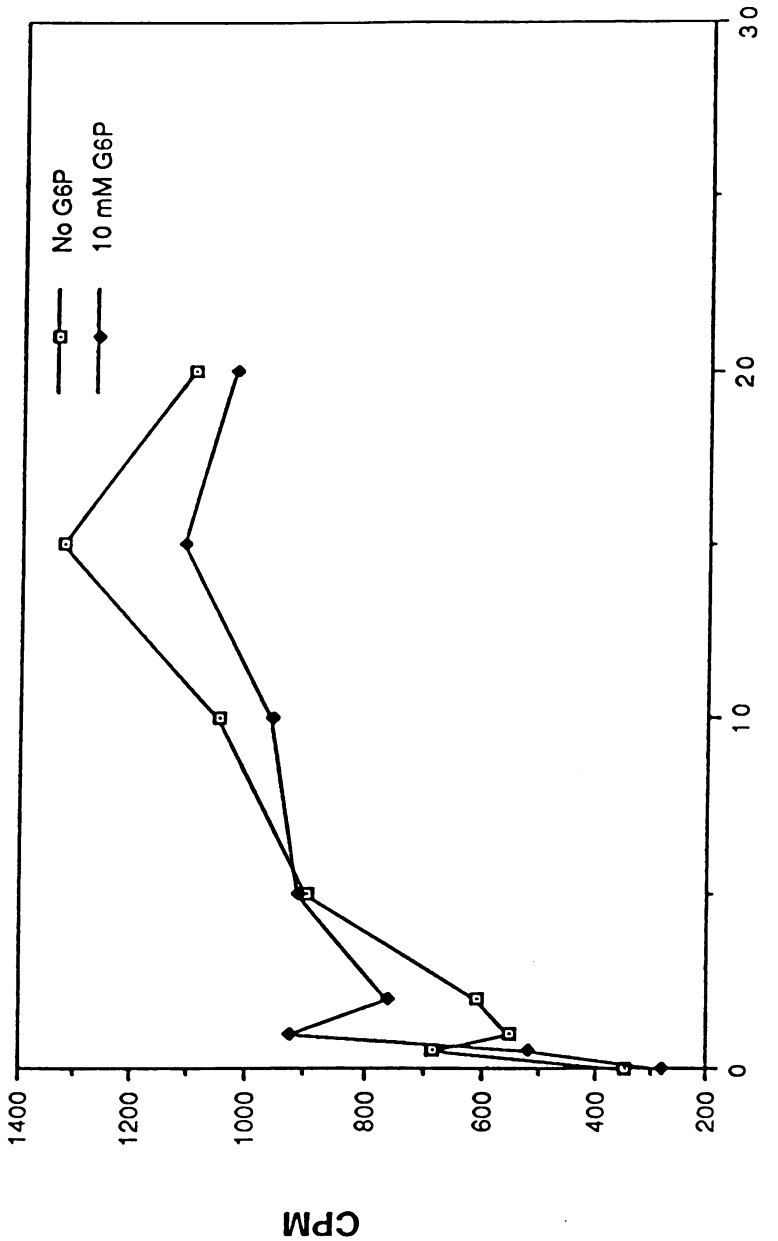
No G6P
10 mM G6P
CPM
1400
1200
1000
800
600
400
200
0
10
20
30
Irradiation time (Minute)

Figure 15

Determination of the incorporation ratio

It was of interest to know how many 3-azido-G6P molecules were incorporated to one hexokinase molecule. From the data of hexokinase concentration determined by absorbance at 280 nm, the radioactivity incorporated into the enzyme, the specific activity of [^{32}P]3-azido-G6P and the molecular weight of hexokinase (about 100 kDa), it is possible to estimate the incorporation ratio. Based on the numerical data in Table IV, the ratio of incorporation was approximately 5-7 molecules of [^{32}P]3-azido-G6P per molecule of hexokinase. This high ratio of incorporation indicated there was nonspecific labeling which labeled the enzyme elsewhere beside the anticipated single binding site.

Scavenging experiment

As noted above, addition of G6P to antagonize 3-azido-G6P binding did not result in any apparent effect based on the labeling observed. Also, considering the high incorporation ratio determined for 3-azido-G6P to hexokinase, there clearly was nonspecific labeling. It was possible that the high amount of nonspecific labeling made specific labeling (if any) difficult to detect. With the hope of eliminating the nonspecific labeling, several scavengers which had been suggested to be useful in other photoaffinity labeling experiments (52, 53) were used in this case.

TABLE IV

THE INCORPORATION RATIO OF 3-AZIDO-G6P TO BRAIN HEXOKINASE

Specific activity of [^{32}P]3-azido-G6P	950 cpm/nmole
Amount of hexokinase in each sample[a]	24.7 μg
Molecular weight of hexokinase	100,000 gm/mole

Sample #[b]	Radioactivity incorporated to the proteins in the sample
Control[c]	131 cpm
1. 5 mM 3-azido-G6P	1795 cpm
2. 5 mM 3-azido-G6 P+10 mM G6P	1361 cpm

	The Incorporation Ratio[d] (molecule of 3-azido-G6P /molecule of hexokinase)
1.	7.10
2.	5.24

[a] The amount of hexokinase was estimated by (Concentration of HK in the irradiated sample) × (Volume of irradiated sample), and the concentration of hexokinase was determined from the absorbance at 280 nm.

[b] Sample 1 and 2 were irradiated at 50 Hz for 5 minutes, but the control sample was not irradiated.

[c] The control sample contained 3 mg BSA and 5 mM [^{32}P]3-azido-G6P

[d] The incorporation ratio was estimated as following,

Moles of hexokinase (A)= amount of HK(gm)/molecular weight of HK(gm/mole)
Moles of 3-azido-G6P incorporated to hexokinase (B)
=[Sample (cpm) -Control (cpm)]/ specific activitry of 3-azido-G6P (cpm/mole)
Incorporation ratio = (B)/(A)

The scavenging experiments were performed under the same incubation conditions as described previously (about 0.3 mg/ml trypsin-modified hexokinase with 6 mM glucose and 5 mM 3-azido-G6P) with the addition of noted concentrations of scavengers. Their effects on labeling were evaluated by SDS-PAGE and autoradiography. The Coomassie blue stained gel and its autoradiogram are both shown in Fig. 16. Lane 1 and lane 2, as indicated, were samples with 10 mM glutathione (reduced form) and their patterns of labeling generally resembled those without additions of scavengers in Fig. 14. The 50 kDa fragment was still most densely labeled with no effect by G6P and the other fragments were still labeled to significant extents, which indicated that glutathione was not an effective scavenger for the radical species generated from photolysis of 3-azido-G6P. Samples with 0.93 mg/ml bovine serum albumin (BSA, about 65 kDa) as scavenger (lane 3 and lane 4) showed intensive incorporation of 3-azido-G6P into the BSA molecules without eliminating the extent of labeling on hexokinase. Thus neither glutathione nor BSA proved to be good scavengers in this experimental system. Allylamine, with unsaturated chemical bonds, was known to react with radicals very readily so it was also used for this scavenging purpose (lane 5 and lane 6). However, its addition resulted in severe degradation of the protein and therefore evaluation of its scavenging effect was impossible.

Figure 16.

The effects of glutathione, bovine serum albumin (BSA) and allylamine as scavengers

The trypsin-modified hexokinase (0.3 mg/ml) was incubated with 6 mM glucose, 5 mM [^{32}P] 3-azido-G6P and varied concentrations of G6P and scavenging molecules as indicated below. All these samples were irradiated with a xenon chloride laser at 50 Hz for 5 minutes. A (top) is the Coomassie blue stained gel, and B (below) is the corresponding autoradiogram of A. Lane 1: no G6P + 10 mM glutathione (reduced form), lane 2: 10 mM G6P + 10 mM glutathione (reduced form), lane 3: no G6P + 0.93 mg/ml BSA, lane 4: 10 mM G6P + 0.93 mg/ml BSA, lane 5: no G6P + 0.21 mM allylamine, lane 6: 10 mM G6P + 0.21 mM allylamine.

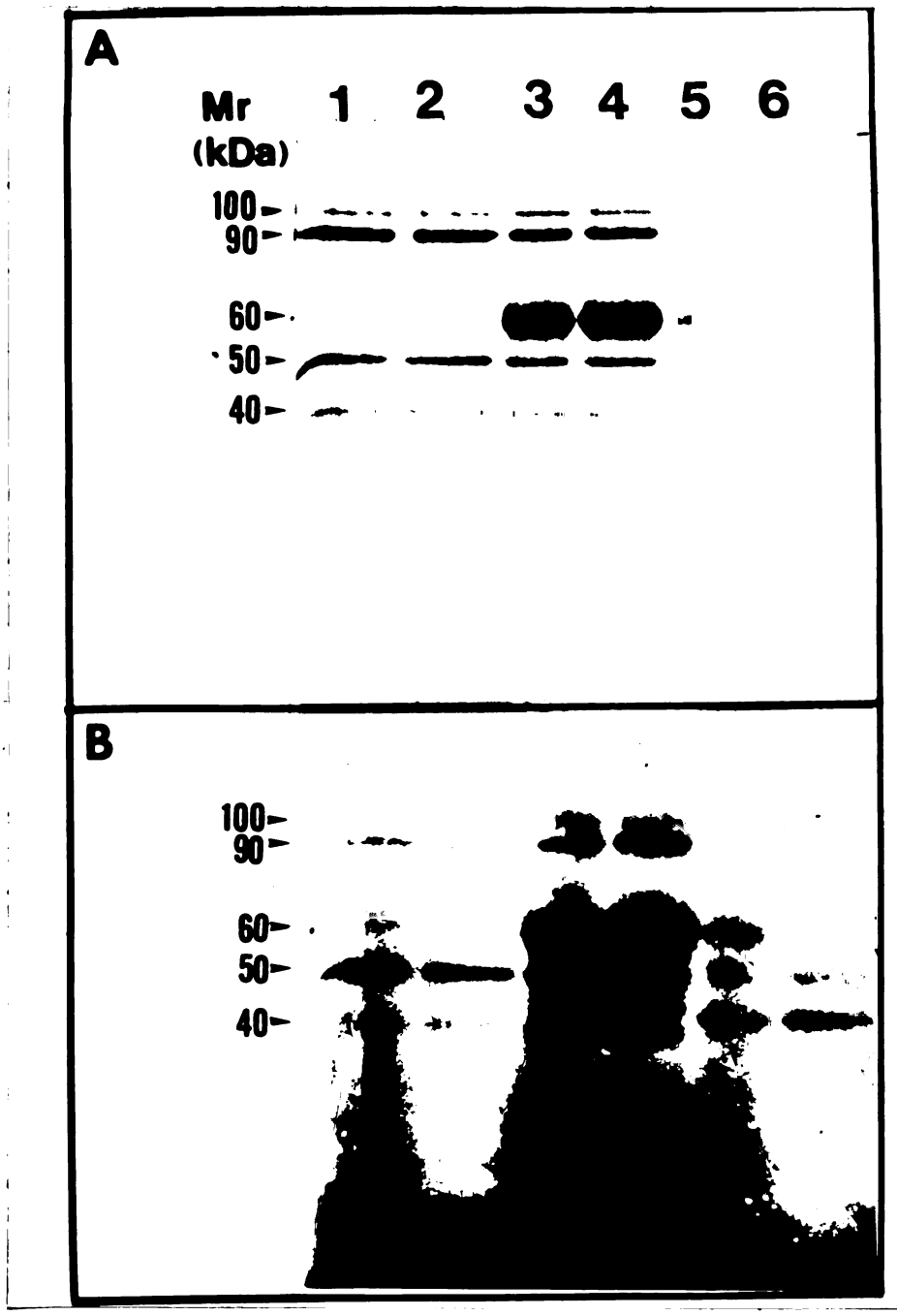

Figure 16

DISCUSSION

Further examination of the specificity for the G6P binding site of brain hexokinase

While designing an affinity labeling reagent for probing the site of interest in a macromolecule, the specificity of the desired labeling site must be considered.

The specificity of the G6P binding site of brain hexokinase has been studied by examining the inhibitory effectiveness of a series of hexose-6-phosphates and related compounds (16, 24, 25). Based on the pioneer studies by Crane and Sols (16), only the hydroxyl groups on carbon 1 and carbon 3 of G6P can be substituted without losing the inhibitory ability on brain hexokinase.

The present work aimed at designing a G6P analog for photolabeling of the G6P inhibitory site of brain hexokinase. Such an analog must contain a photoactivatable group (e.g. azido group) and still behave as a competitive inhibitor (vs ATP) of hexokinase. Based on previous studies (16), substitutions at carbon 2, 4 and 6 of G6P were not considered, since there had marked effect in inhibitory activity. The carbon 1 hydroxyl group of G6P was chosen to be modified; however, β-D-1-azido-G6P and β-D-1-benzyl-G6P were not inhibitors of hexokinase. A mixture of α and β

anomers of either D-1-azidoethyl-G6P or D-1-benzyl-G6P were competitive inhibitors (vs ATP) with the inhibitory effectiveness comparable to the natural inhibitor,G6P. These inhibition results suggested that only α anomers of these G6P analogs were inhibitory, while β anomers were not. Rose et al. (24) have studied the inhibition ability of several G6P analogs with modification at either α or β anomeric positions, and they drew a conclusion that substitution at C-1 equatorial, β, position by groups larger than a proton and smaller than a $-OPO^{2-}$ may prevent binding to the G6P inhibitory site. Also, they suggested the C-1 axial, α, position was free of important steric interactions with the enzyme. The present results are consistent with their suggestions.

Since β-D-benzyl-G6P was not an inhibitor of brain hexokinase, the inhibition by α,β-D-1-benzyl-G6P (70-80% α anomer, with apparent K_i= 0.23 mM) could presumably be attributed to the α form. Even a substitution of the C-1 axial hydroxyl group of G6P with a bulky group as a benzyl group did not affect its inhibition ability, which strongly suggests that there is no direct attachment of the group at C-1 axial position of G6P to the surface of the inhibitory site, and therefore no steric interference with inhibition. Although aryl azides were reported to be more applicable than alkyl azides in photolabeling experiments, it does not seem to be practical to further pursue synthesis of α-D-1-

azidobenzyl-G6P for photoaffinity labeling of the G6P binding site. Even if α-D-1-azidobenzyl-G6P were still an inhibitor of hexokinase by binding at the G6P regulatory site, the azido group on the benzene ring might be far from the surface of the site, so that its photogenerated intermediate would not immediately react with the binding site.

A remaining chance to make an azido G6P derivative with retention of the inhibitory ability would be substitution at C-3 of G6P. 3-Azido-G6P was found to be a competitive inhibitor of brain hexokinase. An azido group was required for photoaffinity labeling and the size of an azido group was very close to that of a hydroxyl group, but a substitution of the C-3 hydroxyl group with an azido group drastically altered the inhibitory effectiveness. The K_i value of 3-azido-G6P was about 10^2 times higher than G6P. This result suggested that there might be fairly close proximity between the hydroxyl group at C-3 of G6P and the surface of the G6P binding site, so that any substituent at the C-3 equatorial position with dimensions larger than a hydroxyl group could result in steric interference and a decrease of inhibitory effectiveness.

<u>The extent of labeling and the problem of nonspecific labeling on brain hexokinase with [^{32}P] 3-azido-G6P</u>

According to the labeling results (see Fig. 14),

significant labeling with [^{32}P] 3-azido-G6P was seen throughout the hexokinase molecule with the strongest labeling in the 50 kDa fragment representing the N terminal half of the molecule. An estimation on the incorporation ratio of [^{32}P] 3-azido-G6P to brain hexokinase (see Table IV) indicated about 5-7 molecules of 3-azido-G6P were incorporated to one moleacule of brain hexokinase after irradiation with a xenon chloride laser at 50 Hz for 5 minutes. Thus it was evident that the present approach met the problem of nonspecific labeling, which has been one of the major difficulties encountered in photochemical labeling studies (53). Although several scavengers were tried for removal of the excess reactive intermediate during photolysis, they did not abolish the nonspecific labeling effectively.

It might not be too surprising that nonspecific labeling occurred in the present labeling experiments. Since 3-azido-G6P (K_i= 2.6 mM) binds to brain hexokinase very weakly, a high concentration (5 mM) was used in an attempt to obtain measurable labeling of the weak binding site. The high ratio of free to bound ligands apparently resulted in a high frequency of bimolecular collisions and therefore nonspecific labeling.

Another possible reason for the nonspecific labeling might be a long-lived photogenerated intermediate or its rearrangement products which diffused from the binding site

and reacted with hexokinase elsewhere beside the specific binding site (54). But nitrenes generated from alkyl azides were reported to be short-lived and rapidly rearrange to imine or amine (55,56). Both imine and amine are nucleophilic species and might react with some functional groups within the hexokinase molecule. In the present experiments, no attempt was made to identify possible long-lived photogenerated intermediates or their rearrangement products, nor to characterize their reactivity toward various amino acid residues.

Speculation about the dense labeling at the 50 kDa fragment with no protection effect by G6P

According to the relative specific activity (see Table III) calculated from the densitometric quantitation of bands on both the Coomassie blue stained gel and the corresponding autoradiogram, it is apparent the 50 kDa fragment derived from the trypsin-modified brain hexokinase was much more strongly labeled with 3-azido-G6P than the other fragments after irradiation.

Since the 50 kDa fragment has been suggested to be where the G6P regulatory site is located (15), it was expected to be specifically labeled with a photoreactive G6P analog, such as 3-azido-G6P. However, in the protection experiment, G6P (10 mM) did not protect the 50 kDa fragment against labeling with 3-azido-G6P. Therefore it was impossible to demonstrate specific labeling of the

inhibitory site.

3-azido-G6P is structurally analogous to the natural inhibitor, G6P, and it was shown to be a competitive inhibitor (vs ATP) of brain hexokinase (Fig. 12). If this analog inhibited the brain hexokinase activity by binding at the G6P regulatory site and inducing a conformational change of the enzyme as G6P, then its specific binding and labeling to the regulatory site should be reduced in the presence of G6P (10 mM). The time course of [^{32}P] 3-azido-G6P incorporation to brain hexokinase (Fig. 15) showed only modest, if any, protection by G6P during the irradiation period. Conceivably the high amount of nonspecific labeling may have obscured specific labeling, i.e., the percentage of specific labeling became very small relative to total labeling. But the dense labeling at the 50 kDa fragment as described previously indicated the total labeling of hexokinase was not just a consequence of random collision between the photogenerated intermediate (from 3-azido-G6P) and the amino residues of brain hexokinase; if it were, all the trypsinized hexokinase fragments would be expected to be uniformly labeled. For some reason still-undefined, the photogenerated intermediate of 3-azido-G6P preferred covalent reaction with the 50 kDa fragment rather than with the other fragments of trypsin-modified brain hexokinase.

The reason for the dense labeling at the 50 kDa fragment was not elucidated in the present work, but possible

explanations for this unusual observation are proposed here.

1. The chemical reactivity of the amino acid residues within brain hexokinase

Nitrenes are assumed to be very reactive radical species that react with almost any functional groups. However, many of the known reactions are efficient only with extremely electrophilic nitrenes or in intramolecular addition (53). For example, it has been found that C-H insertion with aryl nitrenes was very rare, even in the C-H rich hydrophobic core of membranes, and the reaction with nucleophiles was greatly preferred (57,58). The reactivity of aryl nitrenes toward functional groups found in proteins and other macromolecules was summarized by Bayley and Staros (53).

Since alkyl azides were seldom used in photoaffinity labeling of macromolecules, data for chemical reactivity of alkyl nitrenes toward functional groups in macromolecules was not available. Assuming the alkyl nitrenes have the similar reactivity as the aryl nitrenes, then the stronger labeling at 50 kDa fragment could be a consequence of more nucleophilic groups at this fragment than the other fragments of the trypsin-modified hexokinase. However, the complete amino acid sequence of rat brain hexokinase deduced from the cloned cDNA showed extensive sequence similarity between the N- (50 kDa) and C- (40 kDa) terminal halves of this enzyme (59). There were about 49% of amino acids identical and 17% conservative substitutions as the

sequences of these two halves were compared. Therefore, the different extent of labeling at the 50 kDa and 40 kDa fragments could only be explained if the reactivity for the other 34% amino acid constituents of 50 kDa fragment differs from that of the 40 kDa fragment.

2. 3-azido-G6P could bind to brain hexokinase at a site which was distinct from the G6P binding site.

Since 3-azido-G6P is structurally analogous to the natural inhibitor, G6P, and inhibits brain hexokinase in a competitive manner versus substrate ATP as G6P does, it quite possibly binds to brain hexokinase at the G6P regulatory site. But based on the labeling results, G6P failed to show protection effect on brain hexokinase against photolabeling with 3-azido-G6P. Then a question arises, whether the assumption that 3-azido-G6P binds to the G6P regulatory site is correct.

The similarity in structure with G6P and the competitive inhibition of hexokinase activity (vs ATP) might suggest a similar inhibitory mechanism by 3-azido-G6P, but do not guarantee the binding of 3-azido-G6P to the same site where G6P binds. Here 3-azido-G6P is a very poor inhibitor with its K_i value of 2.6 mM, and it perhaps binds specifically to a site at the N-terminal half of brain hexokinase, which is distinct from the G6P inhibitory site.

This possible explanation is consistent with the dense labeling at the 50 kDa fragment by 3-azido-G6P but with no

protection against labeling by G6P.

3. The photogenerated intermediate of 3-azido-G6P might diffuse out of the G6P binding site

Several examples in photoaffinity labeling indicated the photogenerated intermediates could diffuse out of the active site of macromolecules before reacting with other sites (e.g. 54, 60-62). Even when the dissociation constant is low, the diffusion of the photogenerated reactive species still occurs which leads to covalent labeling at a point removed from the active site (63).

Given the apparent low affinity of 3-azido-G6P (K_i= 2.6 mM) for brain hexokinase, it is also possible the photogenerated intermediates of 3-azido-G6P diffuse out of the G6P binding site before covalently reacting with amino acid residues outside that site. Proximity of residues in the N-terminal half to the G6P binding site, also located there, might result in preferential labeling of the N-terminal half.

<u>Suspicion of an unexpected species generated from limited tryptic digestion of rat brain hexokinase</u>

As demonstrated previously (10), the 10, 40, 50 kDa fragments (also the transient intermediates with molecular masses of 60 and 90 kDa) resulting from tryptic cleavage of brain hexokinase remain associated noncovalently, with little change in the kinetic parameters for substrates and

inhibitors. Therefore, it was assumed this trypsin-modified brain hexokinase resembled the native enzyme in structure.

If it were true that tryptic cleavage of brain hexokinase at sites T_1 and T_2 (see p.2) occurred without affecting the native structure, we would expect certain relationships among the relative specific activities (RSA) of the tryptic fragments (as defined in Table III). Thus, it would be predicted that

$$RSA_{90K} = (50/90)(RSA_{50K}) + (40/90)(RSA_{40K})$$

which can be rearranged to

$$RSA_{50K} = (90/50)[RSA_{90K} - (40/90)(RSA_{40K})]$$

Using the RSA_{90K} and RSA_{40K} in Table III, RSA_{50K} is calculated to be about 0.83. However, comparing this calculated value with RSA_{50K} in Table III, the 50 kDa fragment was apparently labeled much more densely (RSA_{50K} is about 1.93) with 3-azido-G6P than expected, and the predicted relationship was not observed.

It is difficult to explain why the 60 and 90 kDa fragments, both containing the 50 kDa fragment in their sequences, were labeled less densely than expected. One possibility is that cleavage at <u>both</u> T_1 and T_2 evokes a conformational change in the 50 kDa fragment which made it

much more susceptible to labeling with 3-azido-G6P.

The utility of alkyl azides in photolabeling of macromolecules

In a review of photoaffinity labeling and related techniques, Bayley and Staros (53) indicated that insertion reactions by alkyl azides, even intramolecular cases, have not been observed because the initially formed singlet nitrene rearranges to an imine (e.g. 55). The only exception at that time was that irradiation of alkyl azides in the lipid bilayer resulted in some insertions into neighboring C-H bonds (64). They suggested this surprising result was perhaps a consequence of constraint on the ability of the singlet nitrene to rearrange into the triplet nitrene in the ordered environment, which leads to the insertion.

Although the present work using an alkyl azide in photoaffinity labeling of hexokinase was not successful in demonstration of specific labeling of the G6P binding site, the photogenerated intermediate of 3-azido-G6P was observed to covalently react with the amino acid residues. Whether this result is a consequence of insertion reactions or of nucleophilic reactions by the rearrangement products (such as imine) was not further explored.

Isolation and analysis of the covalent adducts formed in photolabeling of brain hexokinase with 3-azido-G6P should be useful to give some information in identifying whether there

was insertion reactions by this alkyl nitrene.

One of the problems in utilizing alkyl azides for photolabeling experiments is the inefficiency in photolysis. In the present experiment, this has been conquered by using a laser at the proper wavelength (> 300 nm) as an irradiation source.

Further investigation of the properties of alkyl azides in the context of photochemical labeling may be valuable for their application in biological system.

REFERENCES

1. Wilson, J.E. (1984) in Regulation of Carbohydrate Metabolism (Beitner, R., Ed.), pp 45-85, CRC Press, Boca Raton, FL.

2. Felgner, P.L., Messer, J.L., and Wilson, J.E. (1979) J. Biol. Chem. 254, 4946-4949.

3. Linden, M., Gellerfors, P., and Nelson, B.D., (1982) FEBS Lett. 141, 189.

4. Rose I.A. and Warms J.V.B. (1967) J. Biol. Chem. 242, 1635-1645.

5. Ureta, T., Lazo, P.A., and Sols, A. (1985) Arch. Biochem. Biophys. 239, 315-319.

6. Ellison, W.R., Lueck, J.D., and Fromm, H.J. (1974) Biochem. Biophys. Res. Commun. 57, 1214-1220.

7. White, T.K. and Wilson, J.E. (1990) Arch. Biochem. Biophys. 277, 26-34.

8. Wilson, J.E. (1982) Curr. Top. Cell. Regul. 16, 2-53.

9. Wilson, J.E. (1979) Arch. Biochem. Biophys. 196, 79-87.

10. Polakis, P.G., and Wilson, J.E. (1984) Arch. Biochem. Biophys. 234, 341-352.

11. Xie, G., and Wilson, J.E. (1988) Arch. Biochem. Biophys. 267, 803-810.

12. Schirch, D.M., and Wilson, J.E. (1987) Arch. Biochem. Biophys. 254, 385-396.

13. Nemet-Gorgani, M., and Wilson, J.E. (1986) Arch. Biochem. Biophys. 251, 95-103.

14. White, T.K., and Wilson, J.E. (1989) Arch. Biochem. Biophys. 274, 375-393.

15. White, T.K., and Wilson, J.E. (1987) Arch. Biochem. Biophys. 259, 402-411.

16. Crane, R.K., and Sols, A. (1954) J. Biol. Chem. 210, 597-606.

17. Sols, A., and Crane, R.K. (1954) J. Biol. Chem. 210, 581-595.

18. Casazza, J.P., and Fromm, H.J. (1976) Arch. Biochem. Biophys. 177, 480-487.

19. Solheim, L.P., and Fromm, H.J. (1981) Arch. Biochem. Biophys. 211, 92-99.

20. Lazo, P.A., Sols, A., and Wilson, J.E. (1980) J. Biol. Chem. 255, 7548-7551.

21. Mehta, A., Jarori, G.K., and Kenkare, U.W. (1988) J. Biol. Chem. 263, 15492-15497.

22. Jarori, G.K., Iyer, S.B., Kasturi, S.R., and Kenkare, U.W. (1990) Eur. J. Biochem. 188, 9-14.

23. Hutny, J., and Wilson, J.E. (1990) Arch. Biochem. Biophys. 283, 173-183.

24. Rose, I.A., Warms, J.V.B., and Kosow, D.P. (1974) Arch. Biochem. Biophys. 164, 729-735.

25. Chung, V., and Wilson, J.E. (1989) Arch. Biochem. Biophys. 269, 517-525.

26. Reiser, A., and Wagner, H.M. (1971) in The Chemistry of the Azido Group, pp. 411- 503, Interscience Publishers, a division of John Wiley and Sons.

27. Chowdhry V., and Westheimer F.H. (1979) Ann. Rev. Biochem. 48, 293-325.

28. Scheurich, P., Schaefer, H.J., Dos, K. (1978) Eur. J. Biochem. 88, 253-257.

29. Weber, I.T., Steitz, T.A., Bubis, J., Taylor, S.S. (1987) Biochemistry 26,343- 351.

30. Fleet, G.W.J., Knowles, J.R., Porter, R.R. (1972) Biochem. J. 128, 499-508.

31. Smith, R.A.G., Knowles, J.R. (1974) Biochem. J. 141, 51-56.

32. Saman, E., Claeyssens, M., Kersters-Hilderson, H., and Debruyne, C. (1976) FEBS Lett. 63, 211.

33. Jeng, S.J., and Guillory R.J. (1975) J. Supramol. Struct. 3, 448.

34. Treinin, A. (1971) in The Chemistry of the Azido Group, pp. 25-30. Interscience Publishers, a division of John Wiley and Sons.

35. Bax, A. (1989) Annu. Rev. Biochem. 58, 223-256.

36. Wilson, J.E. Prep. Biochem. 19, 13-21.

37. Chou, A.C., and Wilson, J.E. (1972) Arch. Biochem. Biophys. 151, 48-55.

38. Decker, L.A. ed. (1977) Worthington Enzyme Manual, pp. 221, Worthington Biochemical Corp., Freehold, NJ.

39. Perrella, F.W. (1988) Anal. Biochem. 174, 437-447.

40. Ness, R.B., Fletcher, H.G., and Hudson, C.S. (1950) J. Am. Chem. Soc. 72, 2200-2205.

41. Helferich B., and Weis, K. (1956) Ber., 89, 314.

42. Brimacombe, J.S., Bryan, J.G.H., Husian A., Stacey, M., and Tolley, M.S. (1976) Carbohydrate Res., 3, 318-324.

43. Benson, A.A. (1957) Methods. Enzym. 3, 110-128.

44. Ames, B.N. (1966) Methods. Enzym. 8, 115-118.

45. Treinin, A. (1971) in The Chemistry Of the Azi do Group, pp. 21-23, Interscience Publishers, a division of John Wiley and Sons.

46. Gurst, J.E. (1971) in The Chemistry of the Azido Group, pp. 195-197, Interscience Publishers, a division of John Wiley and Sons.

47. Svennerholm, (1956) J. Neurochem. 1, 42.

48. Smith, M., Moffatt, J.G., and Khorana, H.G. (1958) J. Am. Chem. Soc. 80, 6204.

49. Cleophax, J., Hildesheim, J., Williams, R.E., Gero, S.D. (1968) Bull. Soc. Chim. Fr., 1415.

50. Grossbard, L., Schimke, R.T. (1966) J. Biol. Chem. 241, 3546-3560.

51. Bayley, H., and Knowles, J.R. (1977) Methods Enzymol. 46, 69.

52. Bayley, H., and Knowles, J.R. (1980) Biochemistry 19, 3883.

53. Bayley, H., and Staros J.V. (1984) in Azides and Nitrenes -- Reactivity and Utility, Chapter 9, by Academic Press Inc.

54. Ruoho, A.E., Kiefer, H., Roeder P.E., and Singer, S.J. (1973) Proc. Natl. Acad. Sci. USA, 70, 2567-2571.

55. Kyba, E.P., Abramovitch, R.A. (1980) J. Am. Chem. Soc. 102, 735.

56. Kyba, E.P., (1984) in Azides and Nitrenes -- Reactivity and Utility, chapter 1, by Academic Press Inc.

57. Bayley, H., Knowles, J.R. (1978) Biochemistry 17, 2414.

58. Brunner J., and Richards F.M. (1980) J. Biol. Chem. 255, 3319.

59. Schwab, D,A., Wilson, J.E. (1989) Proc. Natl. Acad. Sci. USA, 86, 2563-2567.

60. Lifter, J., Hew, C.L., Yoshioka, M., Richards, F.F., Konigsberg, W.H. (1974) Biochemistry 13, 3561-3571.

61. Richards, F.F., Lifter, J., Hew, C.L., Yoshioka, M., Konigsberg, W.H. (1974) Biochemistry 13, 3572-3575.

62. Hucho, F., Layer, P., Kiefer, H.R., and Bandini, G (1976) Proc. Natl. Acad. Sci. USA, 73, 2624-2628.

63. Hixson, S.M., and Hixson, S.S. (1975), Biochemistry 14, 4251-4254.

64. Stoffel, W., Salm. K.P., Muller, M., and Hoppe-Seylers Z. (1982) J. Physiol. Chem. 363, 1.